UNIVERSITY OF MINNESOTA
ST. ANTHONY FALLS HYDRAULIC LABORATORY

Project Report No. 294

GROUNDWATER MONITORING NETWORK: ANALYSIS AND DESIGN

by

Roko Andricevic

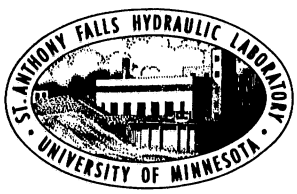

Prepared for

LEGISLATIVE COMMISSION ON MINNESOTA RESOURCES
St. Paul, Minnesota

June 1989

Minneapolis, Minnesota

University of Minnesota
St. Anthony Falls Hydraulic Laboratory

Project Report No. 294

Groundwater Monitoring Network: Analysis And Design

by

Roko Andricevic

Prepared for

LEGISLATIVE COMMISSION ON MINNESOTA RESOURCES
St. Paul, Minnesota

June 1989
Minneapolis, Minnesota

EXECUTIVE SUMMARY

This research presents a methodology for an optimal design of regional groundwater monitoring networks. The design of a monitoring network consists of defining the number, location and measurement frequency of observation wells. The groundwater monitoring program is known to be an expensive, time consuming and uncertain process. Of significant current interest is the problem of developing a sampling plan which will yield information that meets pre–specified criteria set by a decision maker and satisfies budget constraints.

The proposed methodology demonstrates the design and analysis of a regional groundwater monitoring network. The developed technique couples three methods: (1) stochastic groundwater flow simulation with first and second moment analysis to evaluate the effects of parameter uncertainty; (2) variance simulation algorithm for obtaining the variances of the piezometric level estimates at the end of sampling horizon; (3) branch and bound algorithm for solving the mathematical programming problem of finding an optimal monitoring network alternative. A particular attention is given to account for different sensitivity areas in the regional network design. The sensitivity process reveals a different degree of sensitivity for some areas based on future land use and other local parameters related to groundwater management policies. It becomes an important issue for an optimal groundwater monitoring network design. The suggested procedure also provides an optimal spatial and temporal sampling tradeoff. This spatial and temporal consideration of the monitoring network enables a decision maker to optimize a groundwater monitoring network according to the monitoring budget and manpower availability.

The solution for the considered application is obtained from a finite set of chosen network alternatives. The best one is selected as a solution to the mathematical programming formulation. The application results show that the optimal monitoring network depends on the estimate of hydrogeological parameters and their spatial variability. Furthermore, the optimal network strongly depends on the correlation structure of a water table prediction error, which results from the high spatial variability of the aquifer parameters (hydraulic conductivity, storativity and dispersivity).

The developed and demonstrated methodology can be directly used as a tool to design and analyze, in an optimal manner, a groundwater monitoring network quantitatively and/or qualitatively for any site of interest.

ACKNOWLEDGEMENTS

This research was funded by the Legislative Commission on Minnesota Resources.

The figures were drafted by Aaron Gimbel. Abulaban Abdelkarim helped in the construction of the model and Pat Swanson edited the report.

CONTENTS

Table of Contents (Cont'd)

LIST OF FIGURES

List of Figure (Cont'd)

Figure No.

LIST OF TABLES

I. INTRODUCTION

Groundwater monitoring and sampling activity play an important role in the basic needs for human society. Insight into the natural fluctuations of the piezometric levels is gained by measurement programs and by physical laws describing the groundwater movement. Subsurface monitoring is an expensive, time consuming, and uncertain processs. The limited budgets of public agencies usually are unable to support an extensive monitoring program over a long period. Therefore, there is a clear need to develop a monitoring program that is efficient and cost effective.

Until recently, most monitoring wells were placed at more or less arbitrary locations. To obtain information about groundwater behavior, monitoring wells are drilled and piezometric levels measured at the location of the monitoring well. Groundwater velocities and piezometric levels at different locations and times are usually estimated from available measurements. Such an estimation process requires a model in order to relate observed levels at measurement points with levels at any other point in space and time.

A number of philosophies have been proposed over the years for groundwater monitoring network design. There are three most used approaches to analyze and design monitoring networks: optimization, simulation and variance–reduction. Hsueh and Rajagopal [1988] and Loaciga [1988] used an analytical optimization in the selection of sampling sites. The simulation approach was used by Meyer and Brill [1988] and Massmann and Freeze [1987], who focused on the problem of sampling well locations. Besides sampling sites Van Geer [1987] used simulation to account for a temporal sampling, specifying sampling frequency as well. Various other approaches are available in the literature. The mixed–integer programming method, used by Hsu and Yeh [1988] and Carrera et al. [1984], was proposed for sampling aquifer properties. An optimization algorithm was proposed by Szidarovszky [1982], where the optimal measurement point location was selected from a finite set of alternatives. The variance–reduction approach was used by Rouhani [1985]. This is an iterative technique which adds the sampling location which reduces the estimation variance the most. The adding continues until the variance of estimation cannot be further reduced, or when some other constraints are violated.

The objective of this report is to develop a methodology for the design and analysis of a regional groundwater monitoring network used to observe groundwater flow quantitatively. Particular attention will be given for assessing an optimal spatial and temporal sampling tradeoff. The proposed methodology couples three methods: (1) stochastic groundwater flow simulation with first and second moment analysis to evaluate the effects of parameter uncertainty; (2) variance simulation algorithm for obtaining the variances of the piezometric level estimates at the end of sampling horizon;

(3) branch and bound algorithm for solving the mathematical programming problem of finding an optimal monitoring network alternative.

A. METHODOLOGY

The groundwater behavior in the hydrogeologic environment is highly variable (heterogeneous) and average information, the "mean," is meaningless if it is not accompanied by a recognition of the associated error – "variance." There is variability in space due to the heterogeneous hydrogeological characteristics of the porous media (hydraulic conductivity), and variability in time due to non–stationarity of the groundwater flow, particularly where the abstraction is considered. As the land and water resources of a region are developed, different demands will be posed for a monitoring network: data for planning, data for design, and data for use in the water resources system management. Thus, in addition to the variability of hydrogeological phenomena, there is also a variability in conditions for the collection of such data.

As a consequence of the above, the basic questions of groundwater monitoring network design can be summarized with:

1. How many wells ?
2. Where ?
3. How often to measure ?

Because of the uncertainties, both in the form and in magnitude of the subsurface environment and of the future demand prediction, one possible philosophy that a groundwater decision maker might adopt is an attempt to maximize the expected amount of information associated with groundwater quantity/quality over space and time.

In this context, information may be used as a measure of the performance of the groundwater monitoring network. The concept of maximizing the information pertaining to the hydrologic phenomenon of interest was also used by Moss [1986]. Moss and Gilroy [1980] presented an approach, named Kalman Filtering for Cost–Effective Resource Allocation (K–CERA), which enables the decision maker "to determine allocations of the gaging effort among continuous stream gages of the program such that the overall amount of information generated would be nearly maximum."

It is clear that the accuracy of the estimate of the piezometric levels is related to the amount of information available. In particular, if point measurements of piezometric levels are used to estimate the piezometric surface, the information value may be measured by the reduction in the estimation error. This is a general information measure which is also consistent with classical statistical information theory where information is directly proportional to the reciprocal of the spread (variance) of the estimation errors. In order to optimize a groundwater monitoring network in terms of number of wells, location and frequency of measurements, the relationship between the distribution of the information (for given monitoring effort) and losses of the objective has to exist. This means that, generally, an increase of the information must be paid for by an increase in the

monitoring network cost. In practice, however, it is impossible to assess the losses as a function of the reduced information for all relevant future objectives. One reasonable approach to overcome this difficulty is to adopt an Information Reliability Threshold (IRT) value as lower bound. The total information obtained from the network should not fall below this lower bound more than the predetermined probability. This can be expressed mathematically as

$$\Pr \{ [\sigma_i^2]^{-1} \leq \text{IRT} \mid \text{Alt(nw,fr)} \} < \pi \qquad i = 1,...,NN \qquad \text{(I–1)}$$

where σ_i^2 is the variance of the error in the piezometric level at point i, NN is the total number of nodes or elements in the discretized spatial domain and π is the accepted reliability level. The Alt($\cdot$) is an designed network alternative chosen from a prespecified finite set. Each alternative is specified by two network parameters: network density (number of wells–nw) and measurement frequency, fr. Variance simulation algorithm, based on Kalman filtering, is then used to determine the variances of piezometric levels in space and time. The probabilistic constraint (I–1), posed on the variance of the estimation error enables determination of the IRT value, for each selected alternative, which satisfies (I–1).

Note that IRT generally can be a vector. The dimension of this vector may represent areas with different reliability levels assigned. These areas are resulting from a sensitivity mapping process. The sensitivity process reveals a different degree of sensitivity for some areas based on the future land use and other local parameters related to groundwater management policies. The IRT concept, thus, enables decision maker to account not only for the spatial and temporal dimension of a network, but also to account for different reliability levels between subregions.

A finite set of network alternatives can be chosen based on current network performance and on a prior geostatistical analysis which provides the rationale for adding more wells in the proper areas.

This procedure demonstrates the direct possibility of combining different data–collection intensity at a site, distribution in space, and measurement frequency. The spatial and temporal consideration of the monitoring network enables a decision maker to optimize a groundwater monitoring network based on the monitoring budget and manpower availability.

B. REPORT OUTLINE

The chapters which follow present the development and demonstration of the design and analysis of an optimal groundwater monitoring network. In chapter two, the governing equations for groundwater flow and stochastic parameter estimations are presented. The random structure of the log–transmissivity field is employed.

Chapter three focuses on the uncertainty in piezometric levels due to the spatial variability of hydraulic conductivity. To characterize the

uncertainty of model predictions first–order, first and second moment analysis is employed.

In chapter four, an optimization model based on variance simulation algorithm of errors in piezometric levels is presented. The comparison with geostatistical techniques and time series analysis is presented. The rationale for introducing the IRT value with the simulation model is then discussed.

The numerical example which is based on the real field study is the topic of chapter five. The branch–and–bound search procedure is employed to obtain the optimal monitoring network from a finite set of alternatives. The space–time tradeoff is presented and an information scale concept is introduced.

The final chapter contains a summary and conclusions of this study. Some possible extensions and different applications are discussed.

II. MATHEMATICAL DEVELOPMENT

A. STATE–SPACE EQUATION

The groundwater movement in the confined saturated porous medium is described by mass conservation and dynamic (Darcy's law) principles. Many aquifers are commonly modeled with a two–dimensional equation:

$$S\frac{\partial h}{\partial t} = \frac{\partial}{\partial x_i}[T\ \frac{\partial h}{\partial x_i}\ ] + \frac{\partial}{\partial y_j}[T\ \frac{\partial h}{\partial y_j}\ ] + \Sigma Q\,\delta(x-x_i)\delta(x-y_j) \qquad \text{(II–1)}$$

where T is the second rank transmissivity tensor, x_i and y_j are Cartesian coordinates, S is aquifer storativity, Q is the strength of a source/sink, and δ is the Dirac delta function.

The hydraulic response equations of the groundwater system are usually obtained by disctretizing (II–1) in space and solving numerically using finite differences or finite elements. These equations make a system of ordinary differential equations which can be expressed as

$$A\ \frac{dh}{dt} + B\ h + f = 0 \qquad \text{(II–2a)}$$

$$h(0) = h^0 \qquad \text{(II–2b)}$$

The A and B are the coefficient matrices function of the hydrogeological parameters S and T. The f vector contains the sources and/or sinks and boundary conditions of the aquifer system. The h vector is a vector of nodal values of the state variables; the piezometric levels and h_0 are the initial conditions.

If the difference approximation is used to obtain (II–2a) then matrix A is n–dimensional diagonal matrix with elements

$$A_{ij} = \begin{cases} -S_i, & i=j \\ 0, & i\neq j \end{cases} \qquad \text{(II–3)}$$

The B matrix is a function of discretization (Δx) and transmissivity parameter. For steady–state conditions, $dh/dt = 0$ yielding the response equation

$$B\ h + f = 0 \quad \text{or} \quad h = B^{-1}f \qquad \text{(II–4)}$$

The state vector is an explicit function of decision variables contained in the f vector. If we approximate the time derivative using the variable–weighted implicit approximation [Willis and Yeh, 1987] as

$$A\left[\frac{h^k - h^{k-1}}{\Delta t}\right] + B\left[\theta h^k + (1-\theta)h^{k-1}\right] + f = 0 \qquad \text{(II–5)}$$

where θ is the weighting parameter, h^k is the vector of state variables at the k^{th} time level within the planning horizon and Δt is the time step. The state–space equation relates the future piezometric levels to the current piezometric level and boundary conditions. Following this, Eq. (II–5) can be written as

$$[\ A + \theta\Delta tB\ ]h^k = [\ A - (1-\theta)\Delta tB\ ]h^{k-1} - f\Delta t \qquad \text{(II–6)}$$

When θ is one, (II–6) becomes the implicit or backward approximation, when θ is zero the explicit or forward approximation is obtained. The Crank–Nicolson approximation becomes when θ is 0.5. The result may be written in matrix notation as a state–transition equation

$$h^k = \phi\ h^{k-1} + \Psi\ f \qquad \text{(II–7)}$$

The transition matrix ϕ and matrix Ψ depend on the time integration method used. It is clear that ϕ and Ψ may be highly nonlinear functions of A and B, and thus are very complicated functions of the hydrogeological parameters.

The next section will address some techniques which may be employed to estimate unknown system parameters and errors of their estimates.

B. STOCHASTIC APPROACH TO PARAMETER ESTIMATION

Due to the heterogeneity of the geologic formations and processes through which a groundwater system evolves, the hydrogeologic parameters exhibit high spatial variability. The common approach to groundwater flow is to assign the uniform value (often spatial average) to large zones of the aquifer. Unfortunately, the reality shows that aquifers do not have uniform characteristics. The fact that hydraulic conductivity may vary by several orders of magnitude within an aquifer is known from many field studies [Sudicky, 1986]. This spatial variability of hydraulic conductivity is an important factor in modeling the groundwater flow behavior or migration of contaminants. It is also important that uncertainty associated with this variability be incorporated into aquifer models.

To overcome difficulties associated with aquifer heterogeneities, the stochastic approach was used. In this approach, the spatial variability of transmissivity is represented as a random field and described by a probability density function rather than with some average values. The true transmissivity distribution is now considered to be a single realization of the random transmissivity field.

To accomplish the above, the statistical structure of the random transmissivity field needs to be characterized. A full description of the random field would require a knowledge of the joint probability density function for transmissivities at all discrete points throughout the aquifer. It is known that from the single realization it is not possible to infer the joint probability law. This problem can be solved using the assumption of

stationarity. Strict stationarity implies that the joint probability density function is time invariant. In practical applications the relaxed assumption (usually called second order stationarity) is used where only the first two moments, the mean and covariances, are considered stationary. In other words the mean of the random field is assumed constant through space and the covariance at two points, x_i and x_j, depends only on separation distance, r_{ij}. Therefore, throughout this study the transmissivity will be assumed to follow a log–normal distribution, or simply the natural logarithm of the transimssivity, $Y=ln(T)$, is assumed to be normally distributed. The rational for this assumption can be found in Freeze [1975] and Hoeksema and Kitanidis [1985].

Under the above assumption the mean and covariance functions are given as

$$E[Y] = \mu_y \tag{II–8}$$

$$COV_y(i,j) = Q_y(r_{ij}) \tag{II–9}$$

Where $E[\cdot]$ denotes the expectation, COV_y denotes covariance of Y, Q_y is the log–conductivity covariance function, and r_{ij} is the separation distance between spatial locations (x_i,y_i) and (x_j,y_j). Thus, the variance is given with

$$\sigma_y^2 = COV_y(i,i) = Q_y(0) \tag{II–10}$$

Besides the assumption of second order stationarity, it is further assumed that the random log–transmissivity field has an exponential isotropic covariance structure

$$COV_y(i,j) = Q_y(\Delta x_{ij}) = \sigma_y^2 \exp[-r_{ij}/\lambda_y] \tag{II–11}$$

where λ is the correlation scale which is related to the distance at which Y_i and Y_j become uncorrelated. The evidence for assuming the exponential covariance function can be found in Hoeksema and Kitanidis [1985].

Therefore, the heterogeneous log transmissivity field is statistically characterized by the parameters μ_y, σ_y^2, and λ_y. Instead of dealing with numerous distributed parameters and performing extensive calibration (which is often nonunique), the stochastic approach reduces parameter dimension on the above three parameters. Figure 1 shows one such realization of the random log–transmissivity field, generated with mean $\mu_y = 5.2$, variance $\sigma_y = 0.5$, and correlation scale $\lambda_y = 20$ m. The hatched area denotes the transmissivity above and white area below the mean value. The data indicate that the transmissivity can vary several orders of magnitude in natural formations which has also been demonstrated by field studies from Hufschmied [1985] and Sudicky [1986].

The Maximum Likelihood procedure is used in this work to estimate the spatial statisical parameters. This can be accomplished using transmissivity and/or piezometric level measurements. This is the approach first presented by Kitanidis and Vomvoris [1983].

III. UNCERTAINTY IN THE GROUNDWATER FLOW PREDICTION

A. UNCERTAINTY ANALYSIS

In predicting groundwater behavior, there are several potential sources of error. Groundwater flow prediction depends on the spatial and temporal variability in aquifer properties and other hydrogeological parameters. The accuracy and ability to predict groundwater behavior depends on our knowledge of this variability. For the purpose of discussion, uncertainty in groundwater systems may be divided into three categories: modeling errors, aquifer parameter uncertainty, and uncertainty due to spatial variability.

1. Modeling errors

Modeling the reality involves decisions by the modeler how best to describe the hydrologic environment. In each decision there is a certain degree of approximation and simplification. The lack of hydrogeological data or misinterpretation of available data may be one potential source of error in the early stage of modeling. The discretization in space and time associated with numerical modeling represents the errors in the geometry, location of sources and sinks, variations in aquifer properties, etc. All these errors are causing an approximation of the true hydrologic environment. The next possible source of uncertainty is associated with an improper application of these models. For example, using a numerical approximation to the governing equations, proper spatial and temporal discretization is required to avoid the effects of numerical oscillations and round–off error.

2. Parameter uncertainty

The second source of uncertainty in predicting groundwater behavior is an aquifer parameter uncertainty. Model parameters are usually the hydraulic conductivity or transmissivity, porosity, dispersivity, etc. These parameters are never known but rather estimated through a limited number of field and/or laboratory measurements of hydraulic heads, hydraulic conductivity, porosity, etc. Measurements are usually imprecise and parameter estimates will contain many inaccuracies. There is only one true field of aquifer parameter, but it is unknown. Therefore, a probabilistic description of it is often required.

3. Spatial variability

In addition to the errors associated with the estimated aquifer parameters, there is uncertainty due to the spatial variability of these properties. A common approach is to assign uniform values of the aquifer parameters for large zones. Unfortunately, in reality these parameters vary

irregularly and over small distances. In practice, we have only noisy or scarce measurements based upon the characterization of the spatial variability needed. This information uncertainty [Dettinger and Wilson, 1981] is generally reducible through measurement. Thus, optimal monitoring networks should be chosen to satisfy not only the objective about quantity of groundwater, but also to reduce the uncertainty about aquifer parameters and their spatial variability.

B. TECHNIQUES FOR QUANTIFYING THE UNCERTAINTY

Several techniques are available for obtaining the uncertainty in predicted groundwater behavior. Usually we talk about two main groups: full distribution analyses and first and second moment analyses. The full distribution method contains a complete description of the probabilistic properties of aquifer parameters. The derived distribution and Monte Carlo simulation are two of the most important full distribution techniques. The Monte Carlo method is widely applicable and it employs numerous replications of flow system simulation, with the aquifer parameters generated form estimated probability distributions.

The first and second moment analysis is based on the assumption that the mean and the variance–covariance function are sufficient to describe the random variable of interest (in our case predicted piezometric levels). How reliable this assumption is in the practice needs to be checked. However, as stated by Dettinger and Wilson [1981]: "unless the third moment (skewness) or higher moments of the variable are relatively large, they are generally of little interest in application."

Applying first order Tylor series expansion and taking the expected value to numerical solution, of the state–space equation (II–7) for piezometric levels in an aquifer, yields the first order estimate of the mean of h^k:

$$\hat{h}^k = \hat{\phi}\, \hat{h}^{k-1} + \hat{\Psi}\, \hat{f} \qquad \text{(III–1)}$$

where the $\hat{\phi}$ and $\hat{\Psi}$ denote the matrices ϕ and Ψ evaluated at the expected value of the aquifer parameters. If we perform the same procedure for the second moment of piezometric levels, the first order estimate of the covariance of heads at time k is given as

$$P_h^k = \phi\, P_h^{k-1} \phi' + D_t^k\, P_t^{k-1} D_t^{k\prime} \qquad \text{(III–2)}$$

where P_h^k denotes the covariance matrix of the vector h at time k, the prime indicates matrix transpose, and $\mathbf{D}_t$ is the sensitivity matrix defined as

$$D_t^k = \frac{\partial h^k}{\partial t} \qquad \text{(III–3)}$$

what represents the partial derivative of the piezometric levels with respect to the aquifer parameters (e.g., transmissivity). The matrix P_t^{k-1} is the covariance matrix of the generated log–transmissivity field obtained through estimating statistical moments of a single realization of the random field as explained in section II. For more details about random field generation and statistical estimation of the spatial moments, see Appendix A. In order to obtain P_h^k, it is necessary to propagate (II–7) and (III–2) subject to the initial conditions h^0 and P_h^0. To keep this expression for P_h^k simple, it has been assumed that the initial condition h^0 is obtained by interpolating direct measurements of piezometric levels, such that no initial correlation exist between h and t.

Carefully looking at (III–2) it can be seen that the covariance matrix P_h^k is affected by two important correlation scales [Dettinger and Wilson, 1981]. The first one is the correlation length of the uncertain properties at two subsequent times given with transition matrix ϕ. The other is the distance over which the piezometric levels are sensitive to spatially distributed parameters given with sensitivity matrix D_t. Two correlation scales interact so that P_h^k has longer correlation scales than the uncertain parameters. In absence of measurements P_h^k is greater than P_h^{k-1} in most cases. This fact, that the future covariance matrix of the piezometric levels can be reduced by measurement program, will be used to develop the temporal characteristic of the monitoring network.

More generally, if an uncertain aquifer parameter t has covariance P_t, and if piezometric levels h^k are functions of t (and of no other parameters or initial conditions), then following Townley and Wilson's [1984], the covariance of piezometric levels, at some time T, is given to the first order by

$$P_h^T = [D_t^T]\ P_t\ [D_t^T]' \qquad \text{(III–4)}$$

Note that (III–2) is simply the recursive form of (III–4), or one–step propagation uncertainty. Equation (III–4) shows that propagating through time the covariance of piezometric levels depends on sensitivity in heads and covariance of the aquifer parameter uncertainty. In other words the influence of the initial covariance matrix (first term in III–2) disappears gradually. Thus, the covariance matrix P_h^T represents the uncertainty in the predicted piezometric level, at some time T, and will be used in the following chapters as a covariance matrix of the system error term.

IV. OPTIMIZATION OF MONITORING NETWORKS

A. AN OPTIMIZATION APPROACH

In recent years there was an increasing interest in the analysis and optimization of existing monitoring networks and in optimal design of new networks. Monitoring networks provide insight into the groundwater flow for many purposes, for example: water supply, irrigation, dewatering, underground constructions, etc. Since piezometric levels reflect the groundwater behavior, the groundwater system should be deduced from piezometric levels. By using better estimates of piezometric levels, a more efficient groundwater management is possible. Higher accuracy of piezometric levels implies the higher cost of the monitoring network. In this case the optimization follows from compromising between cost of data collection and management and benefits (or losses) for all objectives. To perform this, a very important assumption should exist that there is a relationship between estimation error in piezometric levels and the losses of the objective for which the estimates are used. Better estimates require more wells, better location, or more frequent collection of data. In other words a reduction in the error of piezometric levels must be paid by an increase in the monitoring cost [Van Geer, 1987]. Figure 2 shows this relationship between estimation error and monitoring cost.

B. INFORMATION RELIABILITY THRESHOLD (IRT) VALUE

Unfortunately in reality, it is impossible to optimize a groundwater monitoring network as sketched in Figure 2. The fact that estimated piezometric levels are calculated at particular points in time, while the losses are related to the future, makes it impossible to compare cost and losses at the time the monitoring network should be designed.

As a consequence, it becomes clear that the spatial and temporal aspect of the monitoring network are equally important. Due to the uncertainties in space and time, one philosophy may be to maximize the expected amount of information associated with estimation error of piezometric levels in space and time (Moss, 1986].

Following statistical information theory, the estimation error (or variance) of piezometric levels is related to the information available as

$$\text{Information} = \frac{1}{\text{variance}} \qquad \text{(IV–1)}$$

Such a technology will use, for its objective, the maximization of (IV–1) over space of the variable of interest (e.g., piezometric level). On Figure 3 an "infograph" for piezometric level in an aquifer is depicted. The name infograph comes from the fact that each contour represents a certain degree

of information distributed in the space. It can be seen that the maximization of (IV–1) requires an integration to be carried out over the space and time dimensions. In other words the variance of piezometric levels needs to be evaluated in space and time for solving (IV–1). Of course, this integration process over two spatial and one temporal dimension may easily form a high dimensionality problem.

In this study a new concept is introduced to facilitate the optimal design of the groundwater monitoring network. This concept is represented with probabilistic constraints posed on the estimation error of the piezometric levels and named Information Reliability Threshold (IRT) value. This IRT value for the estimation error variance represents the lower bound, defined such that total information in the area of interest should not fall below more than a predetermined probability (reliability value). Mathematically, this probabilistic statement was represented as

$$\Pr \{ [\sigma_i^2]^{-1} \leq \text{IRT} \mid \text{Alt(nw,fr)} \} < \pi \qquad \text{(IV–2)}$$

where σ_i^2 is the variance of the estimation error of the piezometric level at location i. The rest was introduced in the opening section. On Figure 4 the graphical representation of the IRT value, as a probabilistic constraint (IV–2), is illustrated in terms of the cumulative distribution of the total information. Generally, π can be a vector and the required reliability level can vary from location to location and time to time.

It is important to notice that this formulation of IRT allows different treatment between different subdomains in the area of interest. This is particularly important for the regional monitoring analysis and design. The most common problem with recent techniques for monitoring design is the inability to deal with different sensitivity areas for regional case studies. Sensitivity mapping comes from groundwater quantity and quality and evidently becomes an important issue in the state of Minnesota. Development of the groundwater monitoring network, which will be able to account for different sensitivity in spatial and temporal domain, is the main objective of this study.

Statistically speaking the IRT value can be viewed as e.g., 90 percentile of the distribution of the piezometric level information in one area. Figure 5 shows one possible area of interest and information (inverse variance) associated with each discretized location within this area. Each node has corresponding errors in the piezometric level estimate, quantified with variance of estimation error whose inverse represents the information level at that point in space. Simply, we can find the IRT value such that the total information will not fall below (in this particular area) more than 10 percent. Or, in other words, 90 percent of the information values in that area will be higher than the IRT value. Then, our objective can be to find such network alternatives which will provide the maximum IRT value in the area of interest. The fact that the reliability level π can differ between different subregions enables one to account for different sensitivity areas in the regional groundwater monitoring design. The rationale for reliability of the IRT value comes, thus, from general water management policy, based on technical as well as non–technical decisions.

C. MONITORING NETWORK DESIGN: AVAILABLE TECHNIQUES

In the past, monitoring networks have been used primarily for precipitation, surface water flow, subsurface water flow, etc. Measurements are used to estimate the phenomena of interest. Recently the researchers accounted for errors in these estimates. For example, the decision maker is not only interested in prediction of the piezometric level, but also in the probability of exceeding an arbitrary level. This accuracy of estimation, or particularly standard deviation (or variances), requires stochastic description of the undergoing process. Using stochastic descriptions of the groundwater flow, the influence of the heterogeneity and measurements errors can be analyzed. This analysis has important impact on the optimal monitoring network design. For discussion purposes three groups of methods used in the hydrological network design are described below.

1. Regression Methods and Time Series

Regression methods have a history in applications for the design of precipitation monitoring networks [O'Connell et al, 1979; Bras, 1979). In regression techniques, the analytical function is used to describe the relationship between two or more variables. Parameters of such functions are usually estimated from the measurements in the least square sense. A major difficulty in some applications is to verify the necessary assumption that the measurements of each individual variable are independent.

The estimation of the variable of interest with time series is based on the auto–correlation and crros–correlation functions and estimates can only be calculated for points in time at measurement locations. The auto–correlation denotes correlations between two elements of the same measurement series, while the cross–correlation relates elements of different measurement series. More detailed discussion about time series analysis can be found in Box and Jenkins [1976].

2. Geostatistical Techniques

In order to account for spatial variability there is a need for methods to interpolate the variable of interest between measurement locations. One possible spatial interpolation technique is provided by Kriging [Delhome, 1978]. The Kriging is a method for optimizing the estimate of the variable, which is distributed in space and is measured at a network of points. Until now the Kriging has been used as a spatial interpolation technique for time–independent variables in the area of interest. Estimates of the variable at non–measured locations are estimated as a local weighted average of the observations. The determination of the weights is based on the intrinsic hypothesis, which states:

- The expected value of the variable of interest is spatially independent.
- The variance of the increments is only a function of the distance between two points, and independent of their location.

Information about groundwater flow in time is not used in the Kriging applications, which makes Kriging more statistically oriented and a stationary sampling procedure.

3. Kalman Filtering

The Kalman filtering technique, recently applied (popular in late 70) in hydrology, accounts for temporal and spatial coherence of the process. In Kalman filter applications the description of the flow equations directly enters the calculation. The characteristic that the Kalman filter can be combined with deterministic models in hydrological monitoring network design has been acknowledged by Bras [1978], and Lettenmaier [1979].

In this study, the Kalman filtering technique was adopted for time propagation of the variance of piezometric levels in the area of interest. Note that estimation of the piezometric levels and updating through collected measurements is not needed. The introduction of the IRT value and probabilistic constraint (IV–2) enables one to use the variance simulation algorithm of the piezometric levels in space and time as a function of the certain number of wells and measurement frequencies. In this way the network density and the measurements frequency can be quantified simultaneously. The possibility to change variance of the piezometric levels by changing the measurements frequency is another way to improve the network perfomance. The effect of changing the measurement frequency error (variance) of piezometric levels at some location in space and time is illustrated in Figure 6.

D. VARIANCE SIMULATION ALGORITHM

The variance simulation algorithm is based on the fact that the covariance matrices can be determined without estimating the state vector and without collecting measurements. This fact can be seen from the basic filter algorithm outlined in Appendix B. The simulation filter starts with a stated equation

$$h^k = \phi\, h^{k-1} + \Psi\, f + w^k \qquad \text{(IV–3)}$$

in which a vector w^k denotes the error in the piezometric levels at time k. The rest of (IV–3) is the same as in (II–7). The error term w^k reflects the uncertainty in the predicted groundwater behavior at time k. This uncertainty is due to the parameter estimates and its spatial variability as explained in Chapter III. The error vector is assumed to be zero mean with covariance matrix structure, Q, given with (III–4). This is the place where the system uncertainty due to the heterogeneity of porous media enters the calculation. The covariance matrix Q represents the uncertainty in the predicted piezometric levels as a function of sensitivity matrix D, and the covariance matrix of parameter estimates, P_t. According to (III–4), the matrix Q is time–dependent because the sensitivity is changing with time. Note, furthermore, that this error term may have a non–zero mean value if there is a non–modeled influence in Eq. (IV–3). For example, in a

unconfined aquifer, the recharge due to the precipitation during some seasons can be modeled as average rise of the groundwater due to the precipitation [Van Geer, 1987]:

$$\hat{w}^k = \frac{N_k}{\mu} \qquad \text{(IV–4)}$$

where $\hat{w}^k$ is the average rise in groundwater level, μ is the storage coefficient and N_k is the net percolation. However if we consider that the groundwater flow is modeled correctly, the expected value of the system error is equal to zero.

Together with the stated equation (IV–3), the measurement equation is given as

$$z^k = H_j^k \, h^k + v^k \qquad \text{(IV–5)}$$

where z^k denotes the measurement vector, and H_j^k is the measurement matrix for the j network alternative. The measurement matrix depends on the number of wells and their locations. The measurement matrix may account for possible data missing during the monitoring time. In this case the equation (IV–5) can be easily reduced by dropping the rows of missing data.

The vector v^k denotes the measurement error. With the assumption that the measurement equipment and the observer cause no systematic errors, the expected value of the measurement errors is zero

$$E[\, v^k \,] = 0 \qquad \text{(IV–6)}$$

The covariance matrix R of the measurement error vector v^k reflects the accuracy of the observations. The choice of the matrix R is based on the standard errors produced with the available equipment type. The complete simulation algorithm is given in Table 1 and represents the reduced form of the basic filter algorithm explained in the Appendix B.

The initial condition $P^{0/0}$ can be seen as a sampling spatial error covariance matrix obtained using geostatistical techniques. Each alternative will have different initial conditions based on the number of wells and their location. A time propagation of such defined initial covariance depends on the description of the groundwater flow through the transition matrix ϕ and on the predicted uncertainty modeled with the covariance matrix, Q. Recall that matrix ϕ relates two successive piezometric levels and is evaluated based on the single realization of the random log–transmissivity field.

It is important to notice that the simulation algorithm is obtained without real data. However, the covariance matrix of the piezometric levels do depend on the measurement matrix H_j^k and time step when those measurements will be taken. This fact helps to introduce the finite set of different alternatives (each alternative is described with different number of

TABLE 1.

The Variance Simulation Algorithm

State equation	$h^k = \phi\, h^{k-1} + \Psi\, f + w^k$
Measurement eq.	$z^k = H_j^k\, h^k + v^k$
Prior statistics	$E[v^k] = 0 \quad E[w^k] = 0$
	$E[v^k v^{k'}] = R \quad E[w^k w^{k'}] = Q^k$
	$E[v^k w^{k'}] = 0$
Initial condition	P^0 – known
Simulation algorithm	$P^{k/k-1} = \phi\, P^{k/k}\, \phi + Q^k$
	$P^{k/k} = [I - K^k H^k] P^{k/k-1}$
	$K^k = P^{k/k-1} H^k [H^k P^{k/k-1} H^{k,} + R]^{-1}$

wells, nw, and different measurement frequency, fr, to calculate the variance of the piezometric levels in space and time. Each monotoring network alternative will be propagated with variance simulation algorithm; IRT value, which satisfies the introduced probabilistic constraint, will be determined at the end of the sampling horizon T. In this way the tradeoff between network density and measurements frequency can be obtained. In chapter 5 the numerical example will demonstrate the space–time tradeoff and illustrate how this concept can be used to either improve the existing groundwater monitoring network or design the new one in an optimal manner.

Mathematical Programming Formulation

The final step is to use all of the above to determine the number of wells, nw, their location, and frequency of measurements, fr, such that (1) the maximum IRT value is obtained (total uncertainty in the network is minimized) and (2) the available budget for the network is not exceeded. This can be presented in the mathematical program as follows:

$$\underset{Alt(nw,fr)}{\text{Maximize}}\ C = \sum_{j=1}^{SR} IRT(j) \qquad \text{(IV–7a)}$$

C = total IRT values in the network
SR = number of subregions with specified different reliability level.
Alt(**nw**,**fr**) = finite set of network alternatives as a function of **nw** & **fr**
IRT(j) = information reliability threshold value for the subregion j

Such that:

$$\Pr\ \{\ [P^{T/P}_{i\,i}]^{-1} \leq IRT(j) \,|\, Alt(nw,fr)\ \} < \pi(j) \qquad \text{(IV–7b)}$$

$i=1,\ldots,NN$
$j=1,\ldots,SR$

$$P^{T/T} = [I - K^T H^T]\ P^{T/T-1}$$

$$P^{T/T-1} = \phi\ P^{T-1/T-1}\phi' + Q^T \qquad \text{(IV–7c)}$$

$$K^T = P^{T/T-1} H^T [H^T P^{T/T-1} H^T, + R]^{-1}$$

where T is the sampling horizon, $P^{T/T}_{i\,i}$ denotes the updated variance of the piezometric level at node i, and NN is the relevant number of nodes in the subregion j (see Figure 4). The constraint (IV–7b) is repeated SR times. The K(T) is the Kalman gain matrix and the rest of the variance simulation algorithm terms are explained in Appendix B such that:

$$\text{Budget} \geq T_c = \text{total cost of operating the network} \qquad \text{(IV–7d)}$$

$$T_c = F_c + (\alpha\ \mathbf{nw}) + \sum_{i=1}^{\mathbf{nw}} \beta(i)\ \mathbf{fr}(i) \qquad \text{(IV–7e)}$$

where F_c is a fixed cost which differs from alternative to alternative and depends on well locations and accessability, α is the drilling cost per well, $\beta(i)$ is the cost associated per unit measurement frequency of the i_{th} well, and **fr**(i) is the frequency of the i_{th} well. The cost per unit frequency is assumed to differ from well to well due to the different accessability and distances between observation wells. This completes the mathematical program for the groundwater monitoring design.

The next chapter of the report presents the results of the analysis of one existing monitoring network. The goal is to analyze the current performance of the network and to improve the performance by trading off network density and measurement frequency.

V. APPLICATION

The mathematical programming formulation (IV–7a–e) was used to analyze and determine the optimal network design for one numerical example which is based on experience at an actual field study. The general area is depicted in Figure 7. The site has two water supply wells and five observation wells. There are two natural boundaries and two water courses. Due to the extensive abstraction activity during phase I, the existing monitoring network has been installed to monitor the piezometric level in the area and maintain that level within certain targets. Recently due to the additional agricultural practice in the area and an increased threat from a non–point source pollution, the need for more accurate monitoring has arised. The goal is to improve the existing groundwater monitoring network within the available budget.

A. HYDROGEOLOGICAL SETTING

Due to the lack of necessary field data from the state of Minnesota (author started this research in July 1988), the proposed method will be demonstrated on the site in southern California whose data were available to the author.

The site under study is an area of $3.9 \cdot 4.8$ km^2 in southern California. The elevation of the land surface ranges from about 185 m in the northeast to 105 m in the southwest of the area. The regional basin coincides with two large faults which serve as non–flow boundaries for modelling purposes. There are two water courses: the river in the west and irrigation creek at the east. The level in the irrigation channel is controlled by a number of weirs. Wells drilled in the basin encounter groundwater in sands and gravels ranging from 50 to 120 feet below land surface. Within the basin, groundwater generally flows from the recharge area in the northeast toward the discharge area in the west and south.

1. Identification of Aquifer System and Data Acquisition

The area shown on Figure 7 is located in the central portion of the regional basin. Data collected from phase I demonstrate the existence of one major aquifer system in the alluvial deposits which underlie the site. It follows that that site can be considered as one confined aquifer above an impermeable base. The thickness of the aquifer is estimated at about 55 m. The river on the west side of the site has a strong hydraulic connection with a groundwater flow regime. During the flood season the groundwater flow can easily be reversed.

Data collected from phase I was used to estimate the parameters of the assumed random log–transmissivity field. Piezometric levels were

measured monthly for a period of one year. In addition, pumping tests were conducted to obtain point information about hydraulic properties of the flow at the site. Two pumping tests were conducted at monitoring well three (MW–3) and MW–4 (see Figure 8). The results of these tests are given in Table 2.

TABLE 2

Pumping Test Results in the Area Under Study

Location	Transmissivity	Storage Coefficient
MW–3	770 m^2/d	0.03
MW–4	925 m^2/d	0.01

2. Modelling Effort

The groundwater flow in the area of interest was modeled with a finite difference model (Chapter 2) for one confined aquifer. The site was divided into a rectangular grid in x– and y–directions. The time step was chosen equal to the measurement frequency of 48 times per year. This frequency roughly corresponds to a time step of seven days. An equidistant grid was chosen with $\Delta x = \Delta y = 300$ m. The whole area was therefore divided into 208 square cells of 0.16 km^2 each. The modeled site is depicted in Figure 8. The number of grid nodes for predicting piezometric levels (excluding boundaries) in the x–direction is 15 and in the y–direction 12, yielding 168 grid points.

At each time step, the constant head was assumed at east and west boundaries. The top and bottom of the site under study used the presence of the two faults to assign a no–flow boundary at the north and south portion of the area under study.

Measurements of piezometric levels and transmissivity, obtained through phase I, were used by the maximum likelihood approach to obtain the estimates of the random log–transmissivity field. Table 3 shows the values of estimated parameters at the site. Once the parameter estimates μ_y, σ_y^2, and λ_y were obtained, the characterization of the transmissivity field was fully specified. The transmissivity field was then generated using the turning bands method (Tompson et al., 1987) with statistical characteristics given in Table 3. The generated random field was used to evaluate the matrix ϕ which relates two piezometric levels at successive time steps (Chapter 2). The covariance matrix of the generated parameters was then

employed to evaluate Eq. (III–4) which will serve as a covariance structure for the process error w^k in Eq. (IV–3). This completes the modeling effort to be used with the variance simulation algorithm outlined in Table 1.

TABLE 3

Estimated Values for Hydrogeological Parameters

Method	Parameters		
	μ_y	σ_y^2	λ_y
Maximum Likelihood	6.55 (700 m^2/d)	1.0	120 m

B. PERFORMANCE OF THE EXISTING MONITORING NETWORK

The first part of the solution to the posed problem was analysis of the performance of the existing monitoring network. The current network contains two abstraction wells and five observation wells, all measured with frequency of 12 times per year (monthly). Figure 9 shows the standard deviation surface for errors in piezometric levels obtained with the current network at the end of sampling horizon T. This analysis will serve as a reference for other simulations. Thirteen time steps was needed to obtain the stationary covariance matrix $P^{T/T}$ with the variance simulation algorithm. This plot clearly shows an expected perfomance of the current monitoring network design. The area of high errors will be used as a guidance for selecting the finite set of alternatives which will be considered for the optimization process.

Information Scale Concept

The variance simulation algorithm, introduced in Table 1, is a suitable tool for analyzing the effects of network density and measurement frequency, simultaneously. If the piezometric level is measured in the same observation well, the measurement matrix H_j^k is time invariant, and covariance matrix in $P^{T/T}$ will reach steady values after a sufficient number of time steps. However, if the observation wells are not measured at each time step, the error variances increase during the non–measured period and exhibit a sudden drop at the time of measuring. This fact can be used to compromise between the network density and measurement frequency.

The performance of the existing monitoring network was analyzed through three cross sections. For each cross section the estimation error standard deviation was calculated. Cross sections are shown on Figures 10

through 12. Each of these figures shows four lines corresponding to four successive time steps. The line k=13 corresponds to the time step when measurements are taken, while the rest of lines denote the non–measured time step. Figures 10 and 11 display the estimation error standard deviation increase at the measurement location (node (4,2)) until the new measurement is taken. Moving further aside from the observation well, this difference, between measured and non–measured time steps, disappears and e.g., in the case of cross section A–A on Figure 10, the node (13,2) shows a negligible difference between measured and non–measured time steps. This clearly indicates that the monthly measurement frequency of the existing monitoring network has no effect at a distance more than about 1.2 km.

Notice that this apparent distance depends on the modeling characteristics (Δx,Δy and Δt), on the description of heterogeneity (μ_y, σ_y^2, and λ_y), and on the uncertainty in the predicted piezometric levels described with the covariance matrix Q of the error term w^k. To be consistent with spatial scaling phenomena (e.g., correlation scale λ_y), this characteristic associated with a certain measurement frequency can be named – **information scale**. The importance of this information scale for the network design can be seen from the fact that if two observation wells are separated by a distance less than an information scale, they are providing redundant information for the overlapping area. In other words, the information scale for a certain measurement frequency determines the optimal (in terms of minimal number) spacing for the monitoring well layout.

The west part of the displayed cross section on Figure 10 exhibits a high error in piezometric levels. In other words the total information obtained with the existing monitoring network in this area will be low. Cross section B–B shows the similar pattern revealing, again, the information scale for the existing network. Figure 12 shows the area where there are no observation wells and an influence comes solely from the abstraction well at node (4,10). As expected the error in piezometric levels shows no significant difference between measured time steps and non–measured periods. In the vicinity of the abstraction well a slight influence occurred caused by the information scale when a measurement was taken. Overall this section shows very high error in piezometric levels, and the total information level from this area is very poor.

The difference between the estimation error standard deviation on Figures 10, 11 and 12 indicate that the uncertainty in predicting the piezometric levels in the area of the cross section C–C is much higher than in cross sections A–A and B–B. This can be explained by examining variances of the covariance matrix Q of the error term w^k. The value of the variances are almost doubled in the southern part, indicating a high uncertainty due to the high sensitivity in predicting the piezometric levels in this area.

Note that all the above comments about the performance of the existing monitoring network [13] indicate that the southern part needs more wells and higher frequency of measurements while the northern part might need only higher frequency. The final answer on these questions will be given in the next section where the optimal network design is performed.

C. OPTIMAL SOLUTION BY BRANCH–AND–BOUND METHOD

To optimize the network design and to improve the existing monitoring network, a finite set of alternatives for monitoring network parameters needs to be selected. Rationale for choosing the number of alternatives and the potential location of wells can be found in examining the standard deviation surface for errors in piezometric levels as shown in Figure 9. In areas where the calculated standard deviations are high, one or more observation wells can be added to form a new alternative for the monitoring network. Another direction to achieve a reduction in the standard deviation is to change the measurement frequency at a number of observation wells. Figure 6 shows the effect of changing the measurement frequency on the variance of the estimation error.

The discretization is applied, and a finite set of p alternatives for monitoring networks is selected. Each alternative has two parameters: number of wells, nw, and measurement frequency, fr. The chosen alternatives with corresponding parameters are shown in Table 4. The monitoring network layout is depicted on Figures 14 through 19.

TABLE 4

A Finite Set of Chosen Alternatives

Alternatives	Network Density	Measurement frequency per year
A,B,C	7	12, 24, 48
F,G,D,E	8	4, 12, 24, 48
J,K,H,I	9	4, 12, 24, 48
N,O,L,M,	10	4, 12, 24, 48
R,S,P,Q,	12	4, 12, 24, 48
V,W,T,U,	14	4, 12, 24, 48
X,Y	20	4, 12

The solution to the minimization problem is formulated as

$$\underset{Alt(nw,fr)}{\text{maximize}}\ C = \sum_{i=1}^{2} IRT(i) \qquad \text{(V–1)}$$

such that:

$$\Pr \{ [P_{ii}^{T/T}]^{-1} \leq IRT(j) | Alt(k) \} < \pi(j) \qquad (V\text{–}2)$$

$i=1,\ldots,42$
$j=1,2$
$k=1,\ldots,p$

$$\text{Budget} \geq T_c = \text{total cost of operating the network} \qquad (V\text{–}3)$$

$$T_c = F_c + (\alpha\ nw) + \sum_{i=1}^{nw} \beta(i)\ fr(i) \qquad (V\text{–}4)$$

The monitoring horizon T is one year, and the site has two areas with different sensitivities assigned, as depicted on Figure 20. For the north area the reliability parameter is 5% and for the south, 20%. The total number of nodes is 42 for each sub–area where the information levels need to be computed. The solution of the above problem was obtained by the branch–and–bound algorithm [Fletcher, 1987]. A version of this technique has been previously used by Carrera et al. [1984], to minimize the Kriging variance for spatial sampling design. The details of the branch–and–bound algorithm are discussed next.

The optimal search procedure is based on the monotonic property of the variance simulation algorithm. It is assumed that the sum of variances of the n nodes decreases by either adding an additional observation well or increasing the measurement frequency. This monotonic property of the estimation variances will be used to obtain the optimal alternative by enumeration in a tree search procedure. Figure 21 displays the search procedure for the branch–and–bound algorithm applied in this study. Having in mind that we have a budget constraint (V–3) imposed, the search procedure starts with the current (existing) monitoring alternative. In other words the first node (A) of the tree (Figure 21) corresponds to the current performance of the monitoring network with seven observation wells and measurement frequency of 12 times per year (monthly).

The branch–and–bound algorithm begins at node A and searches the next nodes along the tree branches which will maximize the sum of IRT values (minimize the variances) determined, based on the calculated variances with the simulation algorithm. The search procedure moves forward along the preferential pathway (Figure 21) as long as it improves the objective function (V–1) and satisfies the imposed constraints. Note that the preferential pathway is possible to chose based on the monotonic property of the estimation variance. In other words, if one examines any horizontal row of the search tree from Figure 21, it can be easily seen that the alternative with the highest measurement frequency (48) provides the maximum IRT value. For example, after having computed the IRT values for the alternative at node I, and assuming that all constraints are satisfied, the search procedure continues on the alternative at node M because the alternatives, on the inside branches, F, G, and H would provide the lower IRT value; therefore, there is no need to compute them.

Once the search procedure is interrupted (stopped by violating one constraint), it is then continued at the inside branches of the search tree, until the optimum is reached and constraints satisfied.

1. Discussion of the Results

The described branch–and–bound procedure was applied to the site under study in order to improve the monitoring network performance by trading off a number of additional wells and measurement frequency. The optimal alternative, based on the problem posed by equations (V–1) through (V–4), is one at node L. This is the alternative with 12 observation wells sampled with frequency of 24 times per year or bi–weekly. Figure 22 displays the optimal monitoring network with obtained IRT values. The north sub–area received more wells (three) then the south part (two) due to the different reliability constraints used to illustrate different sensitivity regions. In this particular example the northern area recently experienced an increased agricultural practice, indicating the need to declare this as a higher sensitivity area compared to the rest of the regional basin. It should be noted that the need for different sensitivity areas becomes of high practical importance. A good example may be the movement of the contaminant plume towards the area of water supply or irrigation wells. It is clear that the information obtained from monitoring such areas is important, and the accurate information is almost an imperative. With the IRT value the proposed methodology provides an easy and convenient way to incorporate the decision maker preferences into the mathematical optimization formulation.

Figure 23 displays the standard deviation of errors in piezometric levels obtained with the optimal monitoring network alternative. Comparing this standard deviation surface with one from Figure 9, the clear improvement in terms of the reduction of the estimation variance can be seen.

2. Space–Time Tradeoff and Modeling Error

In chapter 4 the variance simulation algorithm was introduced to calculate the estimation error variances in space and time. The results of the variances calculation are very powerful instruments in the groundwater monitoring network design. The variance simulation algorithm, as shown in Table 1, depends on:

- Measurement accuracy through the covariance matrix, R, of the measurement errors.
- Number of wells and frequency of measurements which is contained in the chosen time step and measurement matrix H.
- Heterogeneity of the hydrogeologic environment through the random description of the log–transmissivity field which affects the construction of the transition matrix ϕ and covariance Q of the system error.
- Model error introduced with the discretization in space and time.

The methodology proposed in this study addresses in detail the first three components above, and the description on how to evaluate this dependence was given in proceeding chapters. The choice of the model was chosen more or less arbitrarily in this report and no influence on the final result from modeling error was investigated in detail. However, as pointed out by Moss [1979] the modeling error can be seen as a third dimension in the network design, and some discussion is left for the end of this section.

The spatial and temporal dimension of the groundwater monitoring network can be generally presented with a space–time contour graph as displayed in Figure 24. Each contour line represents the average standard deviation error of the piezometric level estimates in the area of interest as a function of the network density (determined by the number of wells) and measurement frequency within the sampling horizon. The contours show which combination of the spatial and temporal measurements effort provides the same error in the piezometric level estimate. When the area has a small number of wells, the major improvement obviously results by increasing the number of wells only. The temporal dimension has no significant impact. However, analyzing the network alternatives with number of wells ranging between 5 and 13, the full tradeoff is possible because the equal improvement results from network density and measurement frequency. This was also shown by the solution from the mathematical problem discussed in the previous section.

It is also very important to notice that if we examine the alternatives with the number of wells more than 13, the improvement by adding more wells is only marginal. This can be explained by considering the introduced information scale. Evidently by adding more and more wells we are providing redundant information. Therefore, there is a certain number of wells which can be seen as a "spatial bound" in the network design. In that case, the only significant improvement can be achieved by increasing the measurement frequency. In other words the cost of adding additional wells cannot be justified with gaining additional information from the monitoring network. Unfortunately, in practical applications this fact is almost always neglected.

Notice, however, that the above discussion is somehow conditioned on the chosen model type. As stated by Moss [1979], the model error serves as a control on the space–time tradeoffs that are available to the decision maker. From Figure 24 it seems obvious that there is no practical combination that would improve accuracy in an average sense better than 14 cm. To reach below that level of accuracy, definitely, the better model would be required. Model uncertainty is defined with the covariance matrix Q of the error term w^k in equation (IV–3). A better model can be seen as a model with a finer spatial discretization, which would decrease the covariance matrix Q, and consequently decrease the estimation error variance P_h. The covariance matrix Q was determined based on the uncertainty analysis (chapter III equation (III–4)), and any finer spatial discretization would reduce the sensitivity coefficients yielding a smaller uncertainty overall.

Notice that the model influence on the estimation error variance is present in all interpolation techniques. Therefore, the optimal solution for the groundwater monitoring network always depends on the chosen model.

VI CONCLUSIONS

In summary, a methodology for optimal groundwater monitoring network design has been developed and demonstrated with a numerical example. The proposed method introduced the spatial and temporal dimension of the monitoring network. A finite set of alternatives was selected, and the best one was obtained with a branch–and–bound technique as a solution to the mathematical programming formulation. It was shown that the variance simulation algorithm can be coupled with the stochastic description of the groundwater flow (or transport) to provide a simultaneous tradeoff between the network density and measurement frequency. Theoretical development and application results reveal the following characteristics of the proposed methodology:

- The monitoring network design depends on the hydrogeological parameters description and on the uncertainty which will affect the prediction of the hydrological phenomena.

- The introduced IRT value, in the optimization algorithm, provides the convenient way to account for different sensitivity areas in the regional network design.

- The optimal monitoring network design strongly depends on the correlation structure of an error term w^k in the governing equation. This correlation structure, obtained with a covariance matrix Q, determines the spatial and temporal evaluation of the network, as demonstrated with the introduced information scale concept.

- The formulated mathematical programming problem solved with the branch–and–bound technique, enables a decision maker to obtain the optimal solution from a finite set of alternatives. Notice, however, that this solution is suboptimal because of the choice of a finite set of alternatives.

- It was shown that the model error controls the optimal solution, and can be viewed as a third dimension in the network design. Further research is needed to better quantify and minimize the modeling error impact on the optimal network design.

IX. REFERENCES

Box, G.F.P. and G.M. Jenkins (1976) "Time Series Analysis: Forecasting and Control", Holden–Day, San Francisco.

Bras, R.L. (1978) "Sampling Network Design in Hydrology and Water Quality Sampling", Applications of Kalman filter to hydrology, hydraulics and water resources (ed. Chao–lin Chui). Proceedings of AGU Chapman Conference May 22–24, Pittsburgh, 155–200.

Bras, R.L. (1979) "Sampling of Interrelated Random Fields: The Rainfall–Runoff Case", *Water Resour. Res.*, 15,1767–1780.

Carrera, J., E. Usunoff and F. Szidarovsky (1984) "A Method for Optimal Observation Network Design for Groundwater Management", *J. Hydroogy*, 73, 147–163.

Dettinger, M. and J. Wilson (1981) "First Order Analysis of Uncertainty in Numerical Models of Groundwater Flow, part 1. Mathematical Development", *Water Resour. Res.*, 17 149–161.

Fletcher, R. (1987) "Practical Methods of Optimization", John Wiley, Chichester, England.

Freeze, R.A. (1975) "A Stochastic–conceptual Analysis of One–dimensional Groundwater Flow in Nonuniform Homogeneous Media" *Water Resour. Res.*, 11.

Hoeksema, R. and P.K. Kitanidis (1985) "Analysis of the Spatial Structure of Properties of Selected Aquifers", *Water Resour. Res.*, 21, 563–572.

Hsu, N.S. and W. Yeh (1988) "Optimum Experimental Design for Parameter Identification in Groundwater Hydrology", *Water Resour. Res.*, 25, 1025–1041.

Hsueh, Y.W. and R. Rajagopal (1988) "Modeling Groundwater Quality Sampling Decisions", *Ground Water Monitoring Review*, 121–134.

Hufschmied, P. (1985) "Estimation of Three Dimensional Statistically Anisotropic Hydraulic Conductivity Field by Means of Single Well Pumping Tests Combined with Flowmeter Measurements", in The Stochastic Approach to Subsurface Flow, International Symposium, A.I.R.H. Montvillargenne, France, June 1985.

Kitanidis, P.K. and E. Vomvoris (1983) "A Geostatistical Approach to the Inverse Problem in Groundwater Modeling (steady state) and One–dimensional Simulations", *Water Resour. Res.*, 19, 677–690.

Lettenmaier, D.P. (1979) "Dimensionality Problems in Water Quality Network Design", *Water Resour. Res.*, 15, 1692–1700.

Loaciga, H. (1988) "Groundwater Monitoring Network Design", in Computational Methods in Water Resources, Proceedings of the VII International Conference, MIT, USA.

Massman, J. and R.A. Freeze (1987) "Groundwater Contamination from Waste Management Sites: the Interaction between Risk–based Engineering Design and Regulatory Policy", *Water Resour. Res.*, 23, 351–367.

Meyer, P.D. and E.D. Brill (1988) "A Method for Locating Wells in a Groundwater Monitoring Network Under Uncertainty", *Water Resour. Res.*, 24, 1277–1282.

Moss, M.E. (1979) "Space, Time and Third Dimension (model error)", *Water Resour. Res.*, 15, 1797–1800.

Moss, M.E. and E.J. Gilroy (1980) "Cost–effective Stream Gaging Strategies for the Lower Colorado River Basin", U.S. Geological Survey Open–File Report 80–1048.

Rouhani, S. (1985) "Variance Reduction Analysis", *Water Resour. Res.*, 21, 837–846.

Sudicky, E.A. (1986) "A Natural Gradient Experiment on Solute Transport in a Sand Aquifer: Spatial Variability of Hydraulic Conductivity and its Role in the Dispersion Process", *Water Resour. Res.*, 22, 2069–2082.

Tompson, A.F.B., R. Ababou and L.W. Gelhar (1987) "Application and Use of the Three–dimensional Turning Band Random Field Generator in Hydrology: Single realization Problems", Tech. Report #313, Parsons Laboratory, MIT Cambridge, MA.

Townley, L. and J. Wilson (1985) "Computationally Efficient Algorithms for Parameter Estimation and Uncertainty propagation in Numerical Models of Groundwater Flow", *Water Resour. Res.*, 21, 1851–1860.

Geer, F.C. van, (1987) "Applications of Kalman Filtering in the Analysis and Design of Groundwater Monitoring Network", Tech. Report PN 87–05, TNO–DGV Institute of Applied Geoscience.

Willis, R. and W. Yeh (1987) "Groundwater Systems Planning and Management", Prantice–Hall, Inc., Englewood Clifs, N.J.

APPENDICES

APPENDIX A

The random log–conductivity field used for a single realization problem was normally distributed in the three–dimensional Markov field. In other words, the probability distribution function of ln $K(\underline{x})$ can be defined as

$$\text{pdf} = N(\ln K_g,\ \sigma^2) \tag{A–1}$$

where N denotes the standard normal distribution, and K_g is the geometric mean conductivity:

$$K_g = \exp \langle \ln K \rangle \tag{A–2}$$

where $\langle \cdot \rangle$ denotes the expectation operator, and σ^2 is the variance of the log–conductivity perturbation. The covariance function of this random field has exponential form:

$$R(\xi) = \sigma^2 \exp(-\sqrt{\textstyle\sum_i \xi_i^2/\lambda_i^2}) \tag{A–3}$$

where ξ_i is the separation vector, and λ_i is the correlation scale of the log–conductivity along the principal axis x_i (i = 1,2,3). In the special isotropic case ($\lambda_1=\lambda_2=\lambda_3$), the covariance function takes the simple form:

$$R(\xi) = \sigma^2 \exp(-\xi/\lambda) \tag{A–4}$$

where ξ is the separation distance, and λ the isotropic correlation length (same in all directions).

The statistical estimation for the spatial moments of single realizations of random fields was based on standard spatial average estimators applicable under the assumption of spatial homogeneity and ergodicity.

The discrete spatial moments of the prescribed log–conductivity field were computed by using standard unbiased estimators:

$$\text{Mean} = \ln \hat{K}_g = \frac{1}{N} \sum_{i,j} \ln K_i, \tag{A–5}$$

$$\text{Variance} = \hat{\sigma}^2 = \frac{1}{N} \sum_{i,j} \langle k(\underline{x})^2 \rangle \tag{A–6}$$

where N is the total number of nodes on the grid ($N = n_1 n_2 n_3$), and k is the log–conductivity perturbations. The covariance function was evaluated in a similar fashion:

$$\hat{R}(i_1,0) = \frac{1}{N(i_1)} \sum_{j_1,j_2} k(j_1,j_2) \cdot k(j_1-i_1,j_2) \qquad (A-7)$$

where $N(i_1)$ denotes the number of pair of points with separation vector $\xi = (i_1\Delta x_1, 0)$ on the grid, that is:

$$N(i_1) = (n_1-i_1) \cdot n_2 \qquad (A-8)$$

Note that $0 \leq i_1 \leq n_1-1$. The indices j_1 and j_2 in (A-7) was from (1,1) through (n_1-i_1,n_2).

APPENDIX B

This Appendix presents the general form of the Kalman filter algorithm for linear and non–linear systems. The objective of the Kalman filter algorithm is to calculate the optimal estimate of the state vector at each time step k from:

- all measurements up to time k
- initial conditions
- measurement covariance matrix
- system noise covariance matrix

In addition to the optimal estimate of the state vector at time k, the covariance matrix of the estimation error of that estimate is calculated.

The starting points of the derivation of the Kalman filter algorithm for linear system are:

- a system described by the state transition equation:

$$x(k+1) = \phi(k)x(k) + w(k) \tag{B–1}$$

- a measurement process which can be described by the measurement equation:

$$z(k+1) = H(k+1)\, x(k+1) + v(k+1) \tag{B–2}$$

where x(k) is the nx1 state vector, z(k) is the px1 measurement vector, w(k) is the system noise vector, v(k) is the measurement error vector and $\phi(k)$, $\psi(k)$ and H(k) are known matrices. Further it is assumed that:

$$E[w(k)] = 0\ ,\quad E[v(k)] = 0 \tag{B–3}$$

$$E[w(i)w^T(j)] = \begin{cases} Q(i), & i=j \\ 0, & i\neq j \end{cases} \tag{B–4}$$

$$E[v(i)v^T(j)] = \begin{cases} R(i), & i=j \\ 0, & i\neq j \end{cases} \tag{B–5}$$

$$E[v(i)w^T(j)] = 0\ ,\ \text{all i and j} \tag{B–6}$$

The resulting Kalman filter algorithm is given in the table below.

system equation: $x(k+1) = \phi(k)x(k) + w(k)$ measurement equation: $z(k+1) = H(k+1)x(k+1) + v(k+1)$
Initial conditions: $\hat{x}(0/0)$ and $P(0/0)$

Filter algorithm

Time update (effect of system dynamics)

error covariance: $P(k+1/k)=\phi(k)P(k/k)\phi^{T}(k)+Q(k)$
estimate: $x(k+1) = \phi(k)x(k/k)$

Measurement update (effect of measurements)
error covariance:

$$P(k+1/k+1)=[P^{-1}(k+1/k)+H^{T}(k+1)R^{-1}(k+1)H(k+1)]^{-1}$$

estimate: $x(k+1/k+1)=x(k+1/k)+K(k+1)[z(k+1)-H(k+1)x(k+1/k)]$

where K(k+1) is the Kalman gain matrix given as

$$K(k+1) = P(k+1/k+1)H^{T}(k+1)R^{-1}(k+1)$$

In the case with nonlinear system dynamic the Extended Kalman Filter (EKF) was used. The nonlinear functions, if sufficiently smooth, can be expended in Taylor series about the current best estimates x(k/k). Retainning the first two terms and assuming knowledge of x(k/k) enables us to use the following table.

System model and measurement model:

$$x(k+1) = f(x,k) + w(k)$$

$$z(k+1) = h(x,k) + v(k)$$

$$w(k) \approx \{0,Q(k)\},\ v(k) \approx \{0,R(k)\}$$

Assumptions:

w(k) and v(k) are white noise processes uncorrelated with x(0/0) and with each other.

Initialization:

$$x(0/0),\ P(0/0)$$

Time update:

estimate: $x(k+1/k) = f(x(k/k),u,k)$
error covariance: $P(k+1/k) = A(x,k)P(k/k) + P(k/k)A^{T}(x,k) + Q(k)$

Measurement update:

estimate: $x(k+1/k+1)=x(k+1/k) + K(k+1)[z(k+1) + h(x(k+1/k),k+1)]$

error covariance: $P(k+1/k+1) = [I - K(k+1)H(x,k+1)]P(k+1/k)$

Jacobians:

$$A(x,k) = \frac{\partial f(x,u,k)}{\partial x}$$

$$H(x,k) = \frac{\partial h(x,k)}{\partial x}$$

FIGURES 1 THROUGH 24

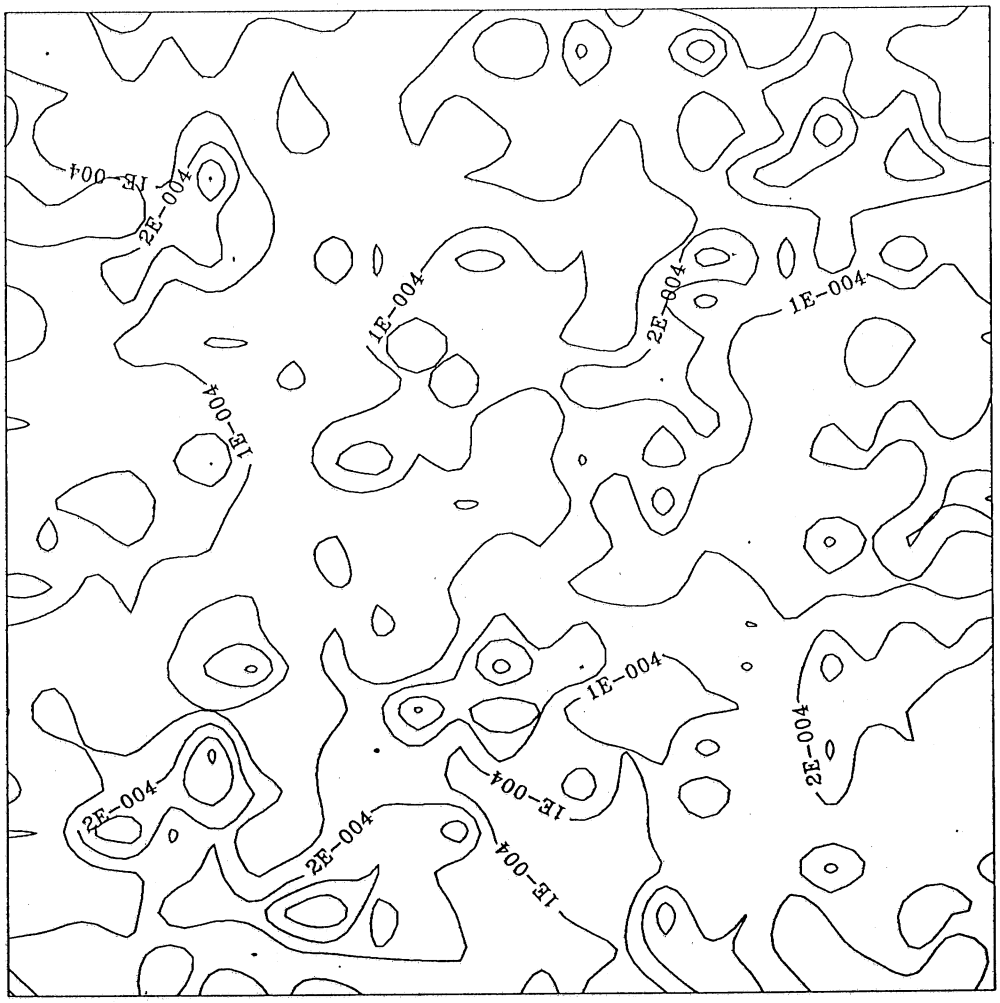

Fig. 1 Typical realization of the log–conductivity field.

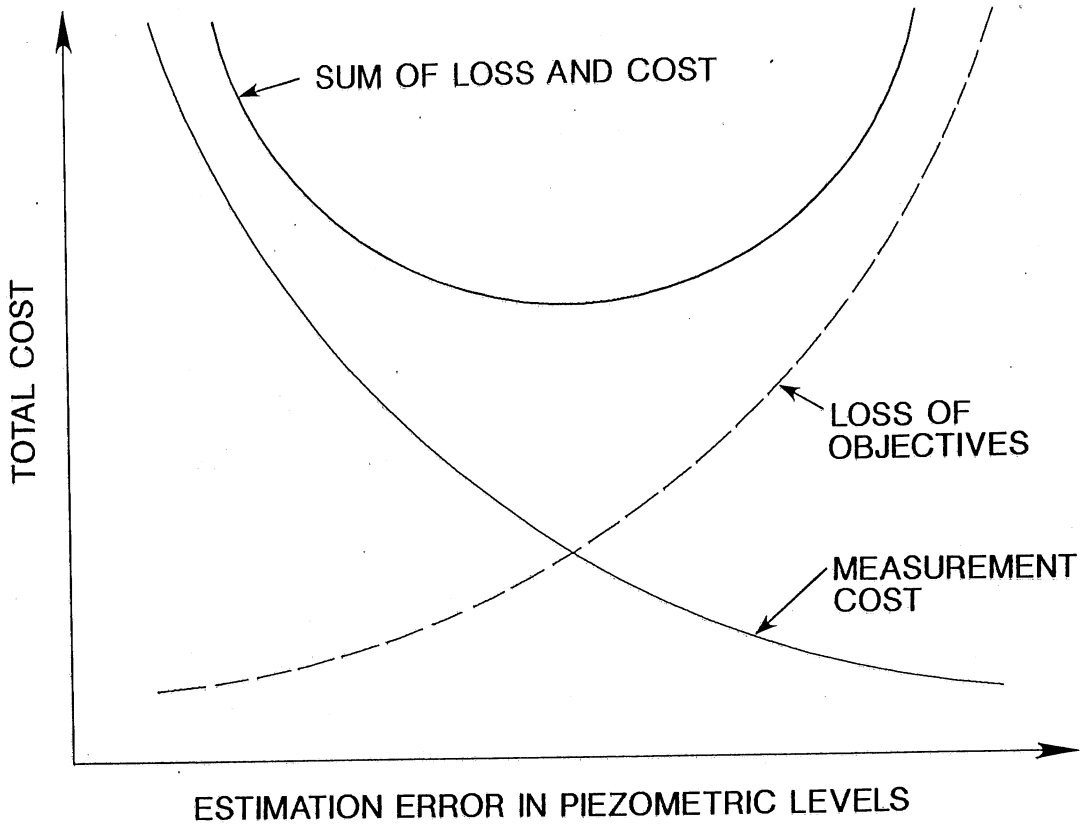

Fig. 2 Relationship between estimation error and monitoring cost.

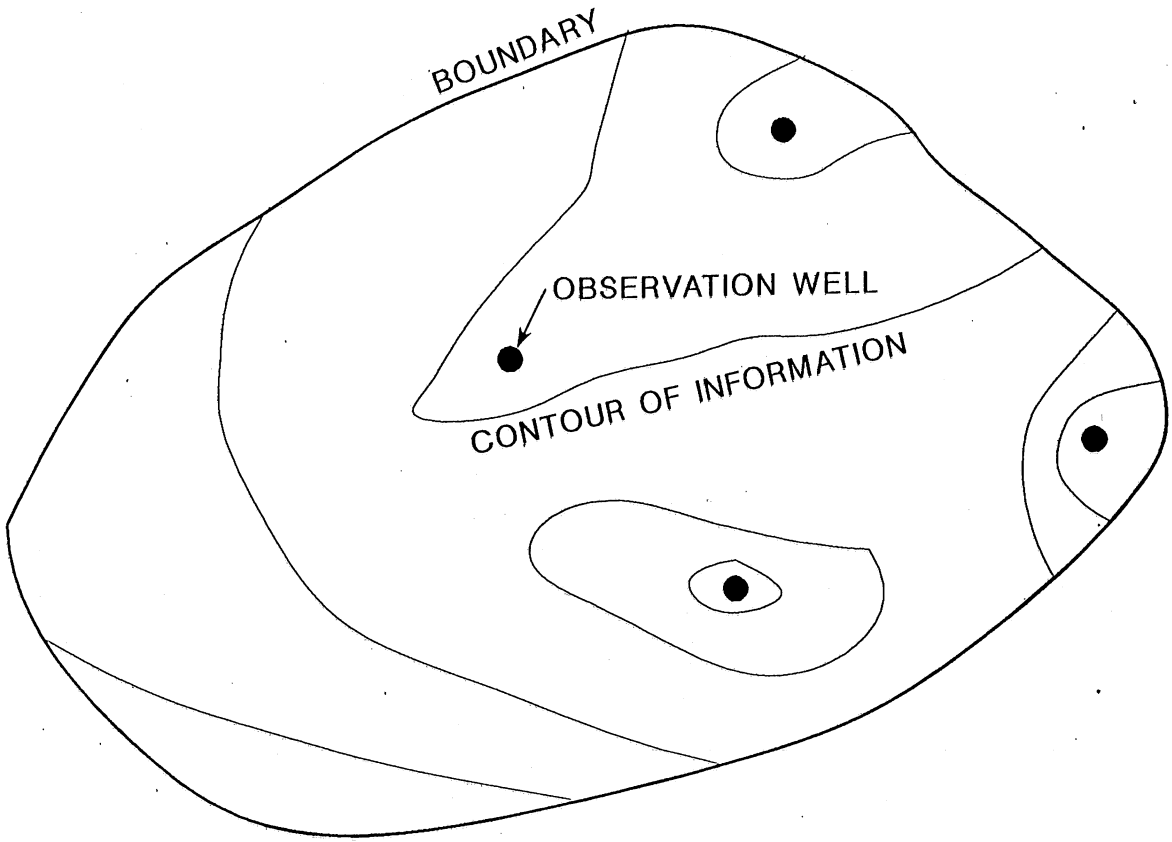

Fig. 3 Typical infograph for piezometric levels of a hypothetical aquifer.

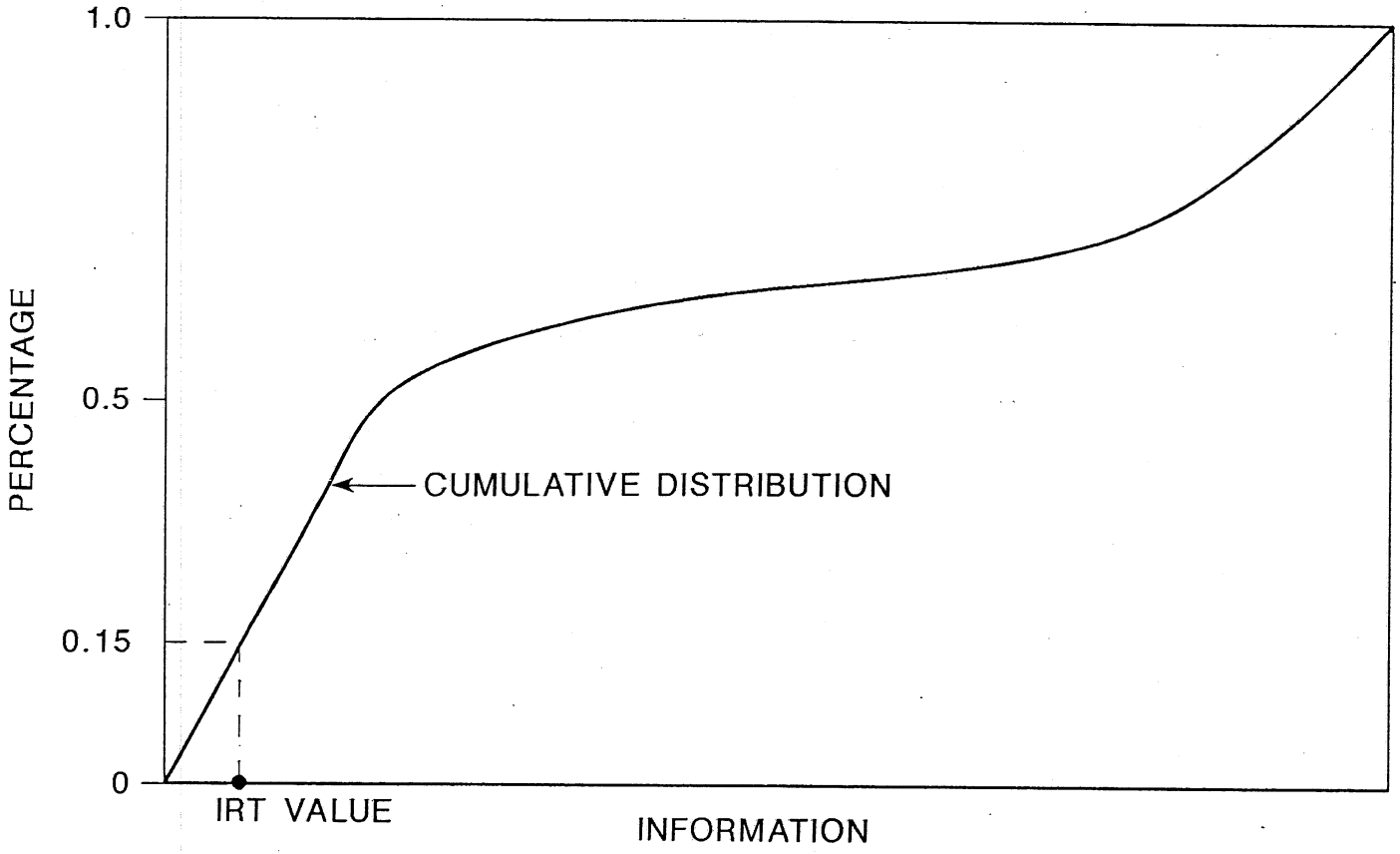

Fig. 4 Graphical representation of the IRT value.

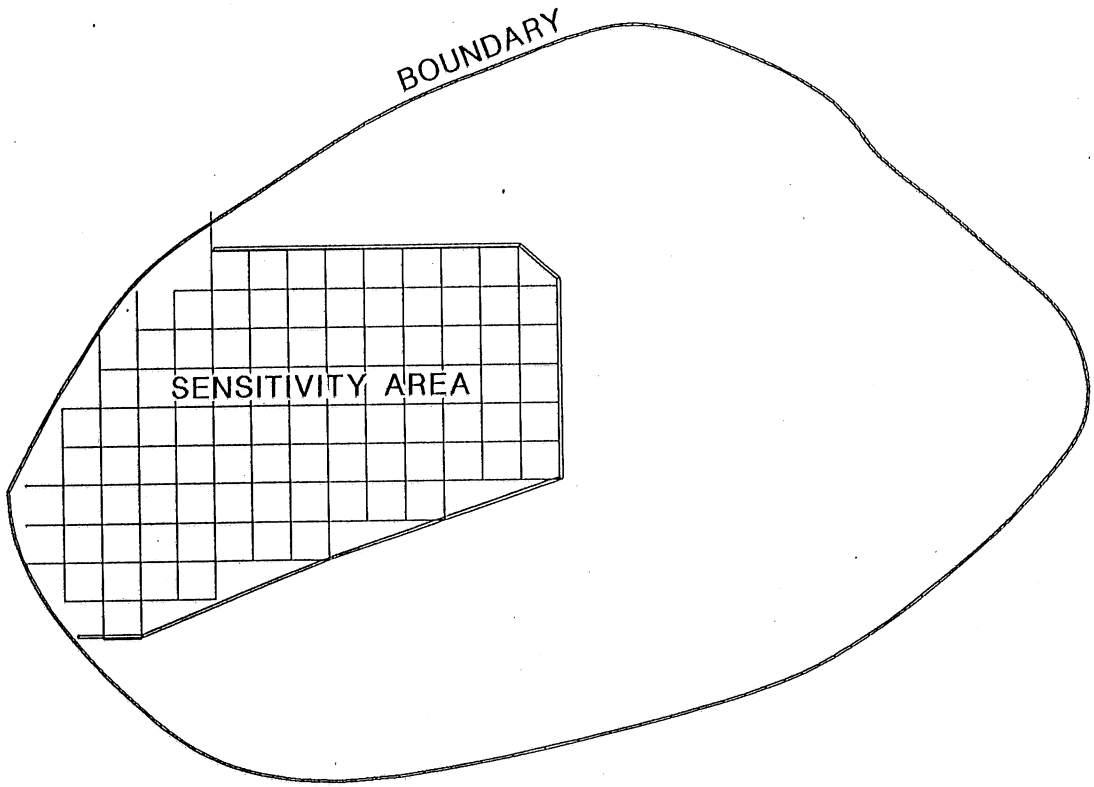

Fig. 5 Typical area of a different sensitivity level.

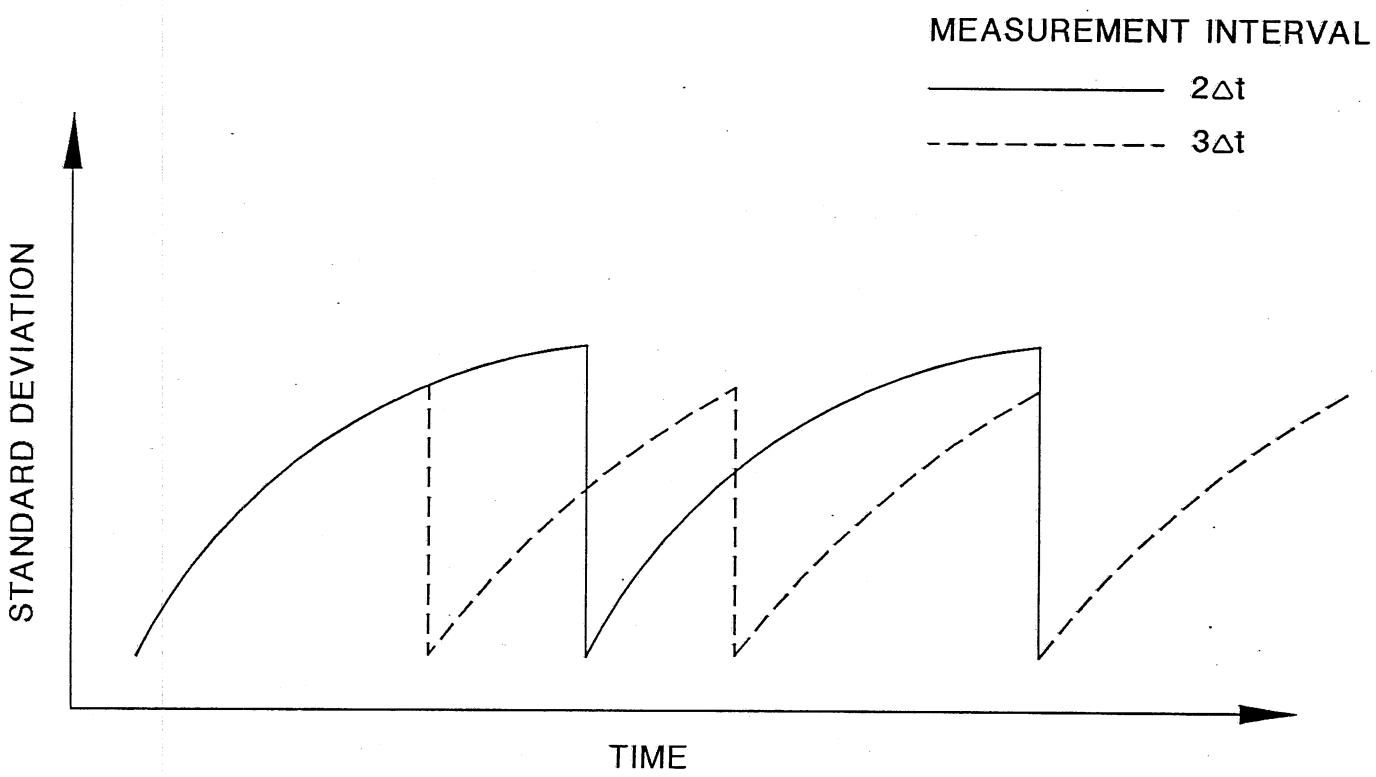

Fig. 6 Effect on changing measurement frequency on the estimation error variance.

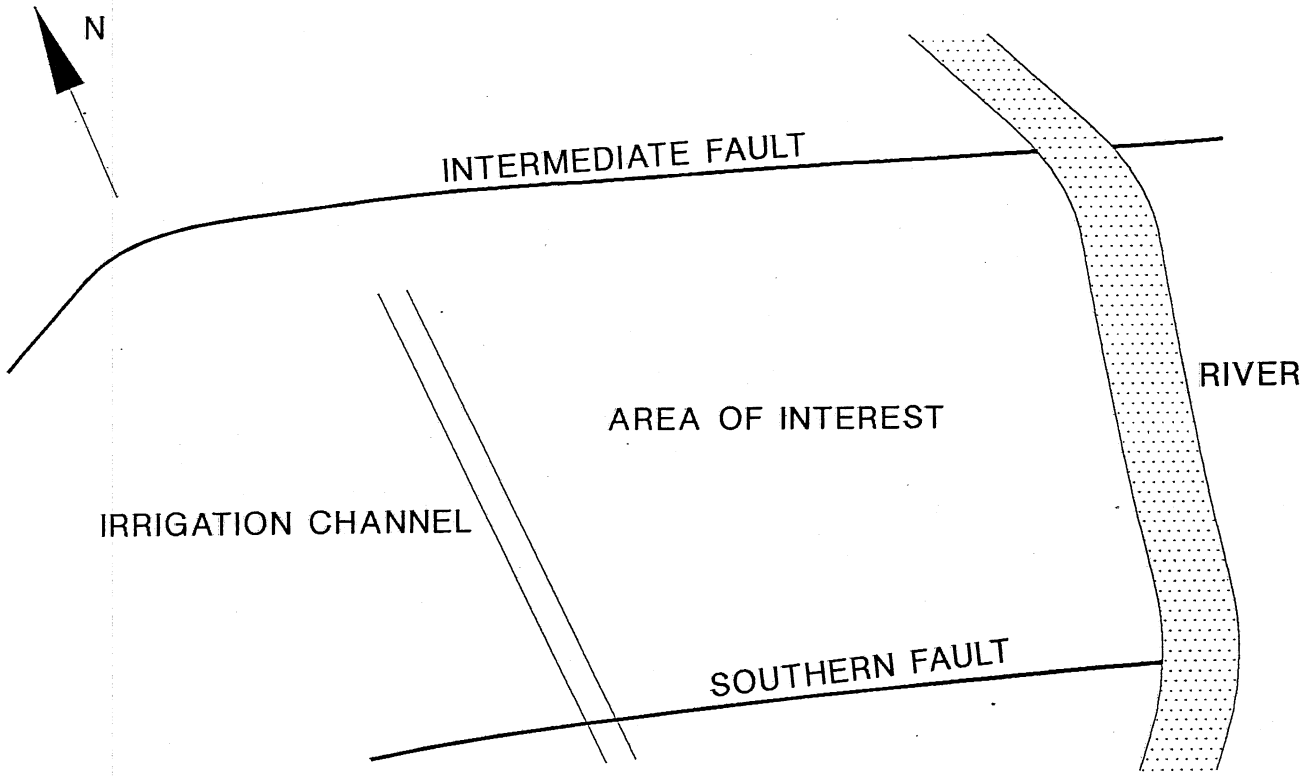

Fig. 7 The regional basin under study.

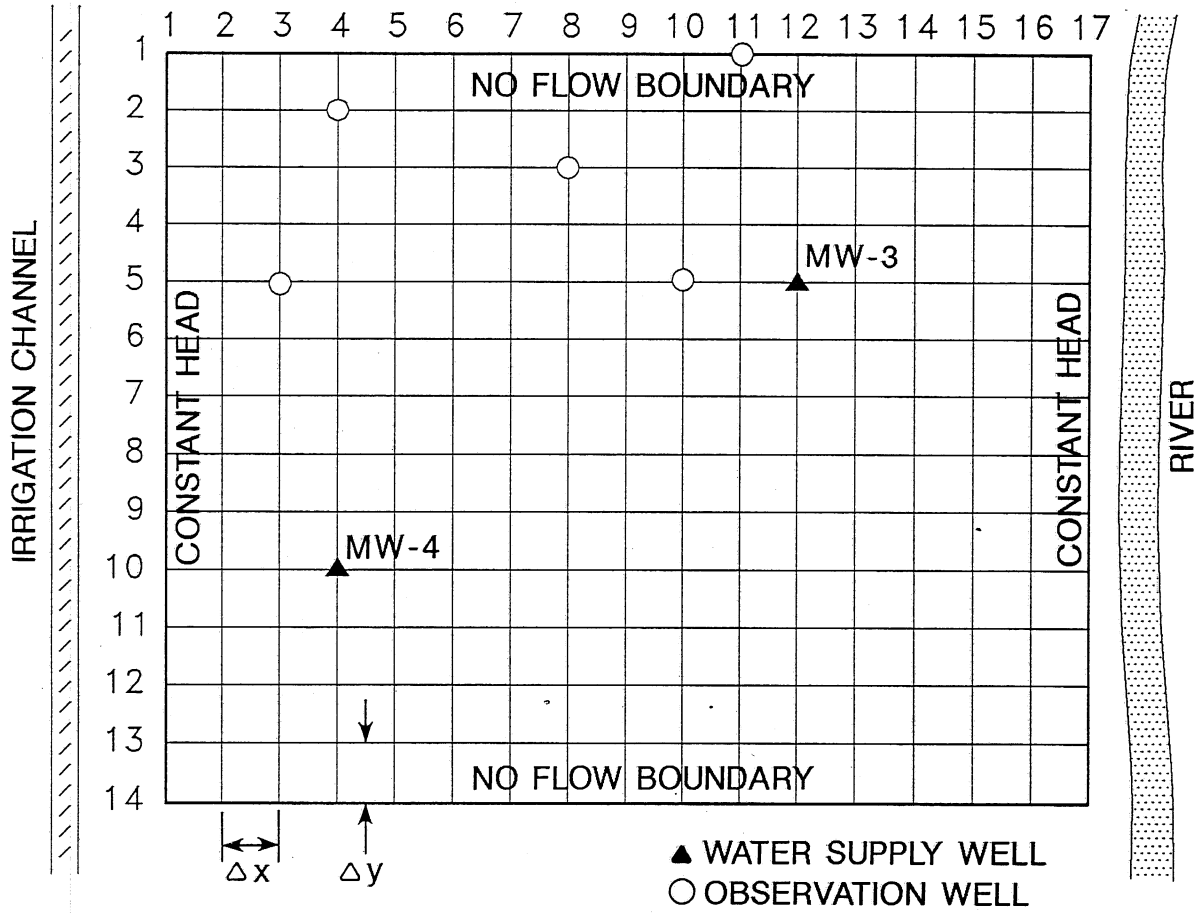

Fig. 8 The numerical model for the area of interest.

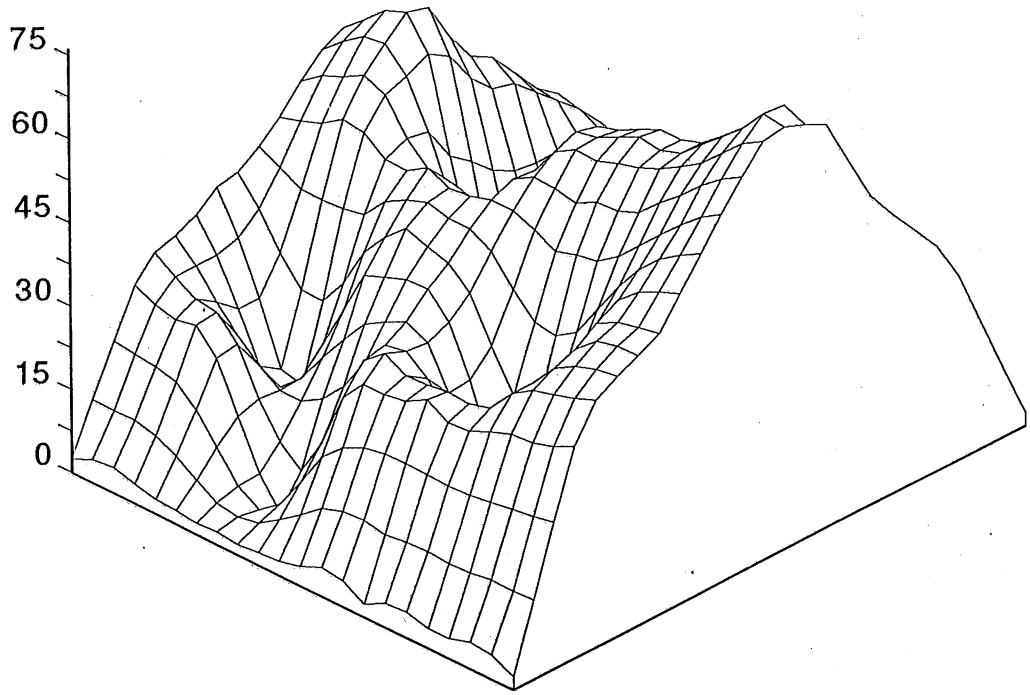

Fig. 9 The error standard deviation surface for existing monitoring network.

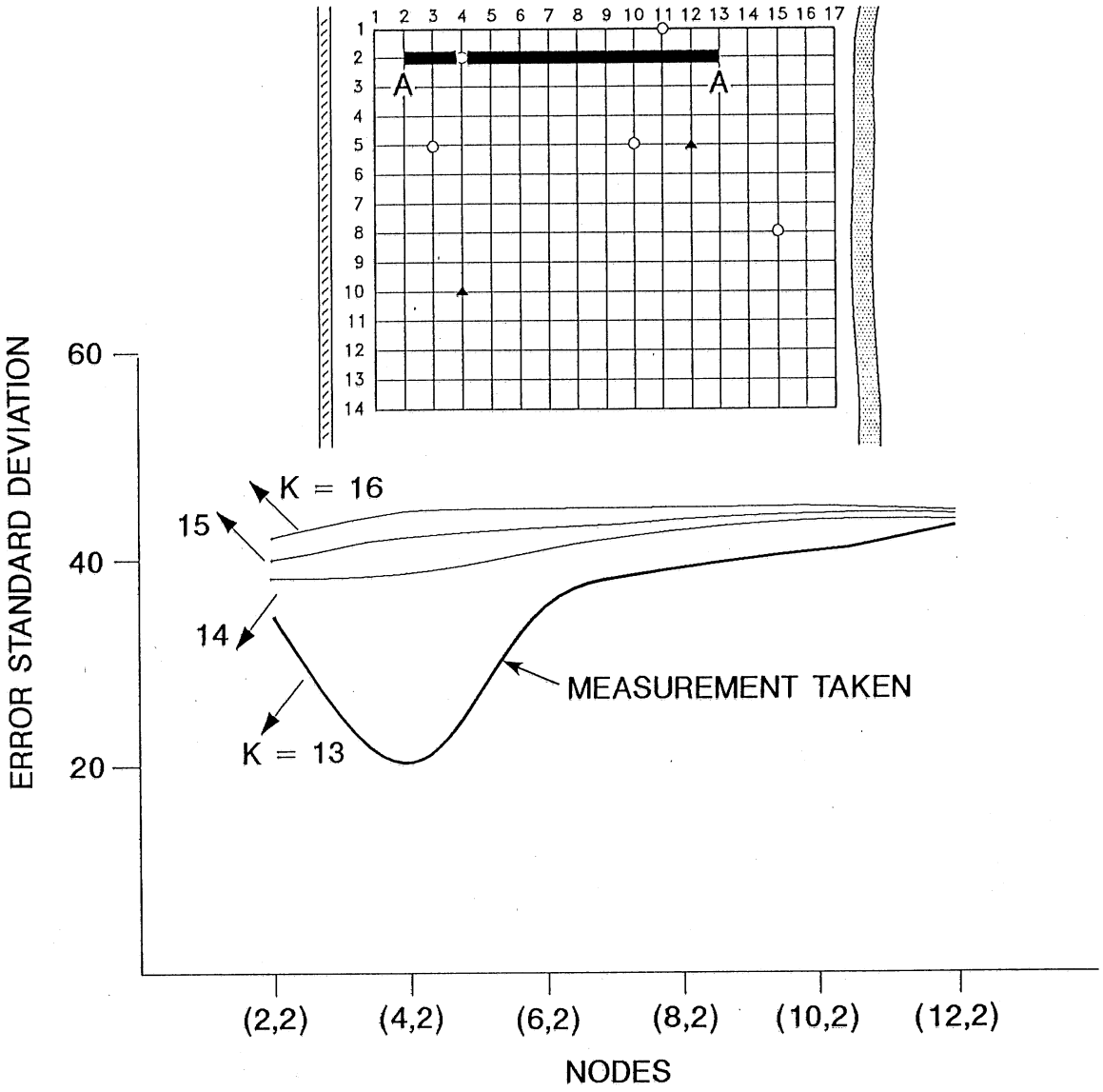

Fig. 10 The error standard deviation for cross section A–A.

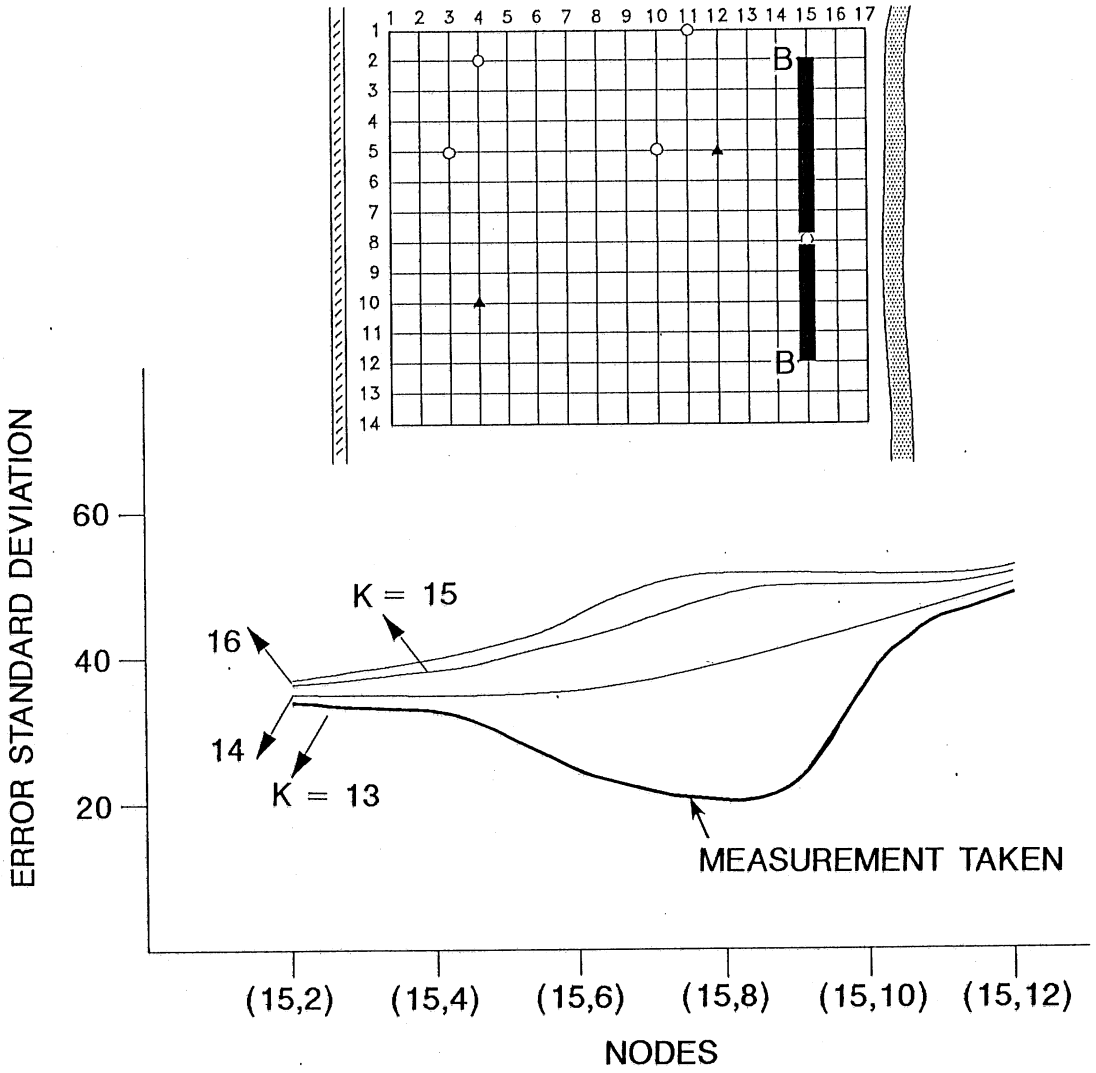

Fig. 11 The error standard deviation for cross section B–B.

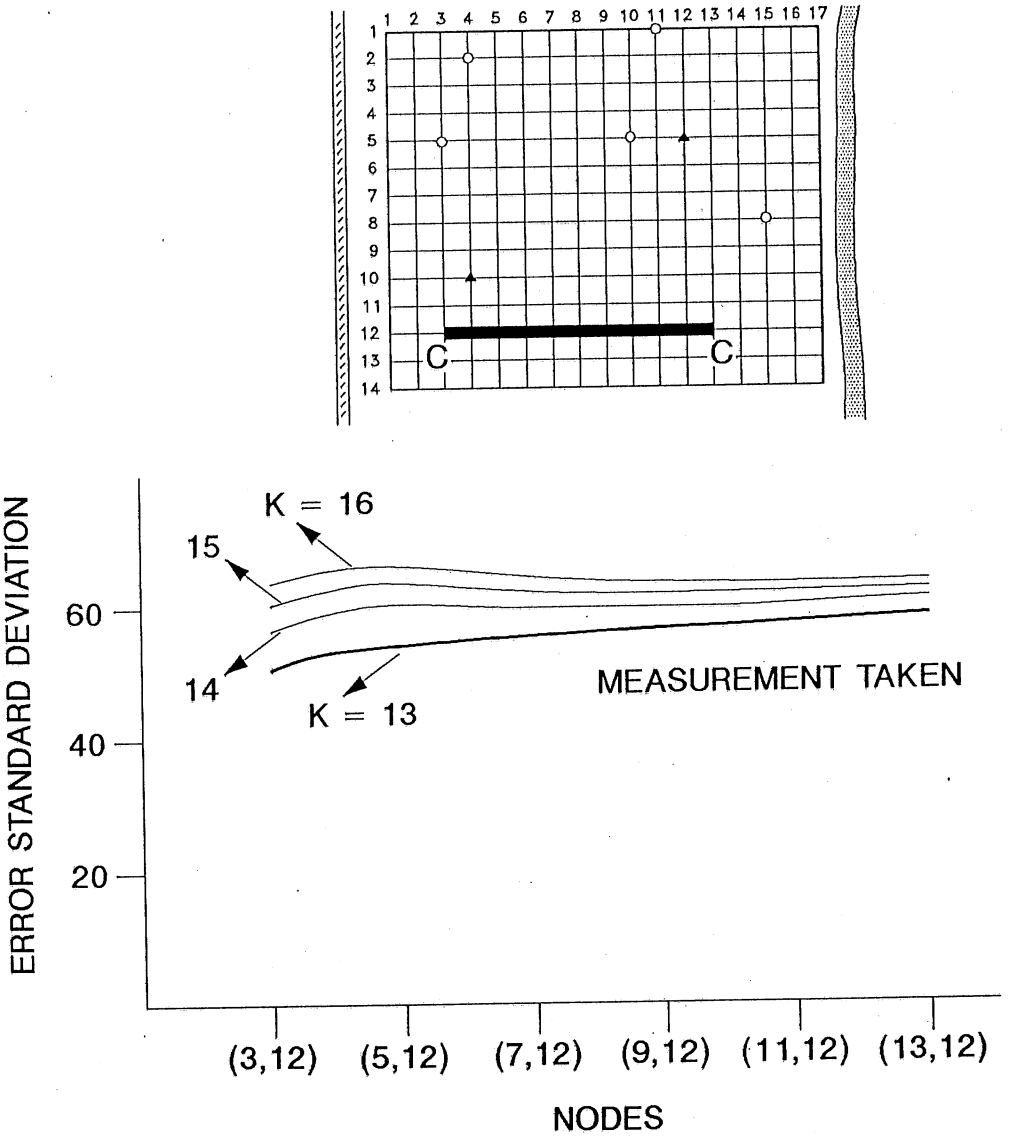

Fig. 12 The error standard deviation for cross section C–C.

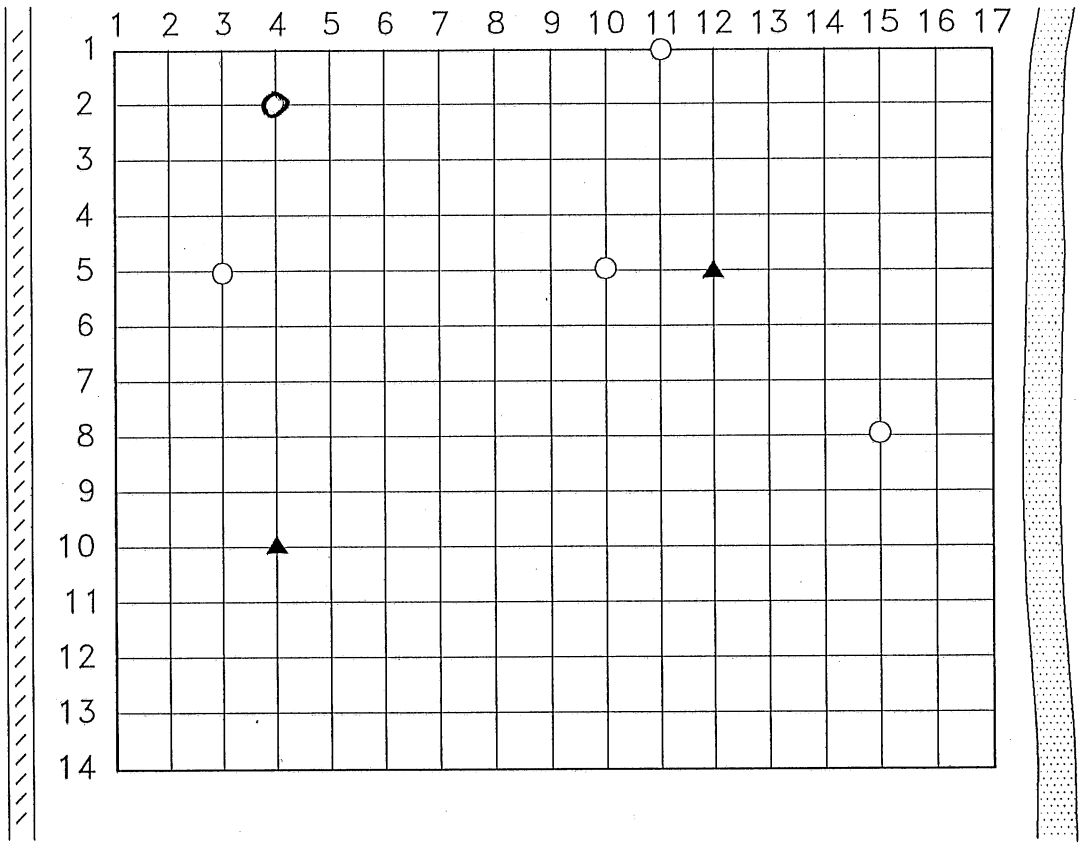

Fig. 13 Existing groundwater monitoring network.

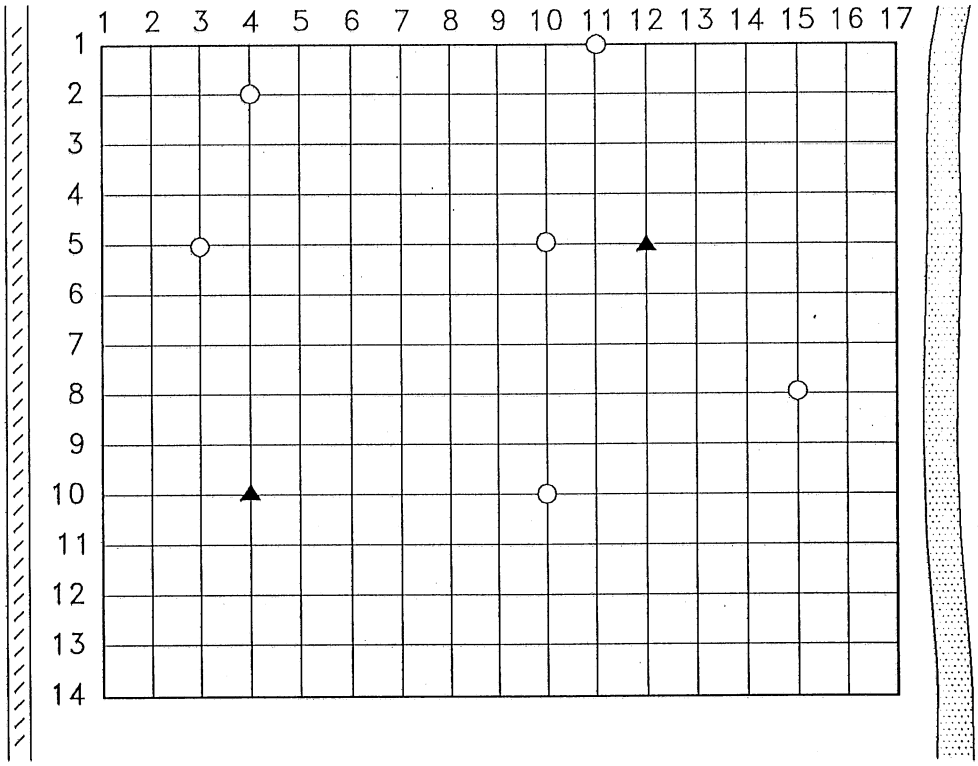

Fig. 14 The alternative with 8 monitoring wells.

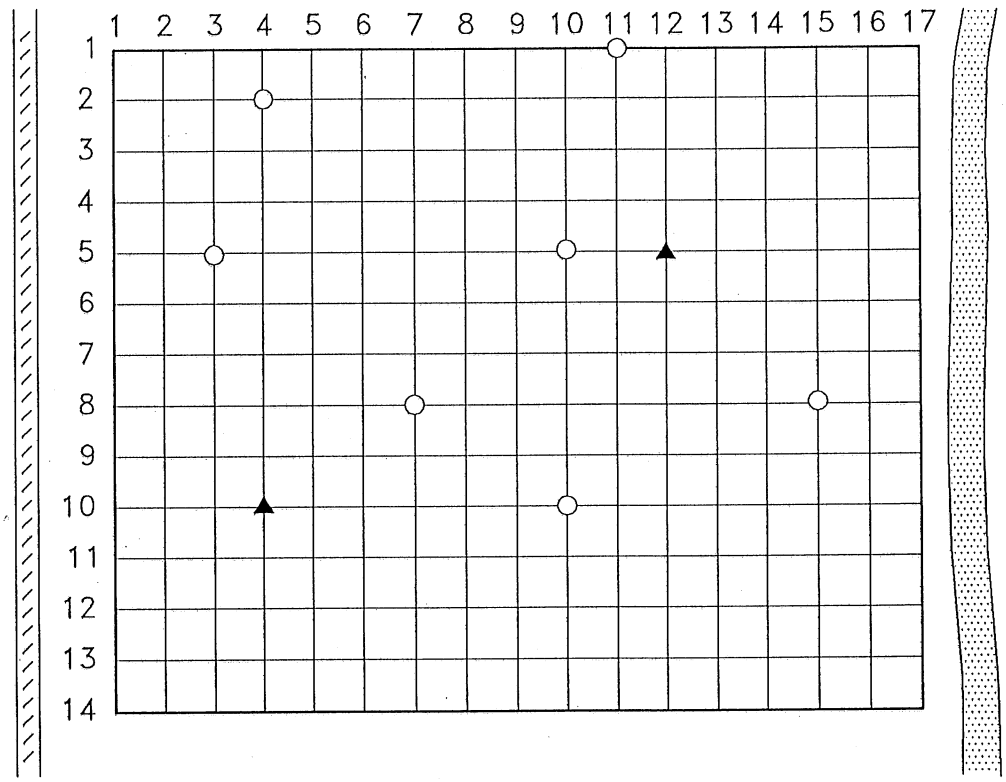

Fig. 15 The alternative with 9 monitoring wells.

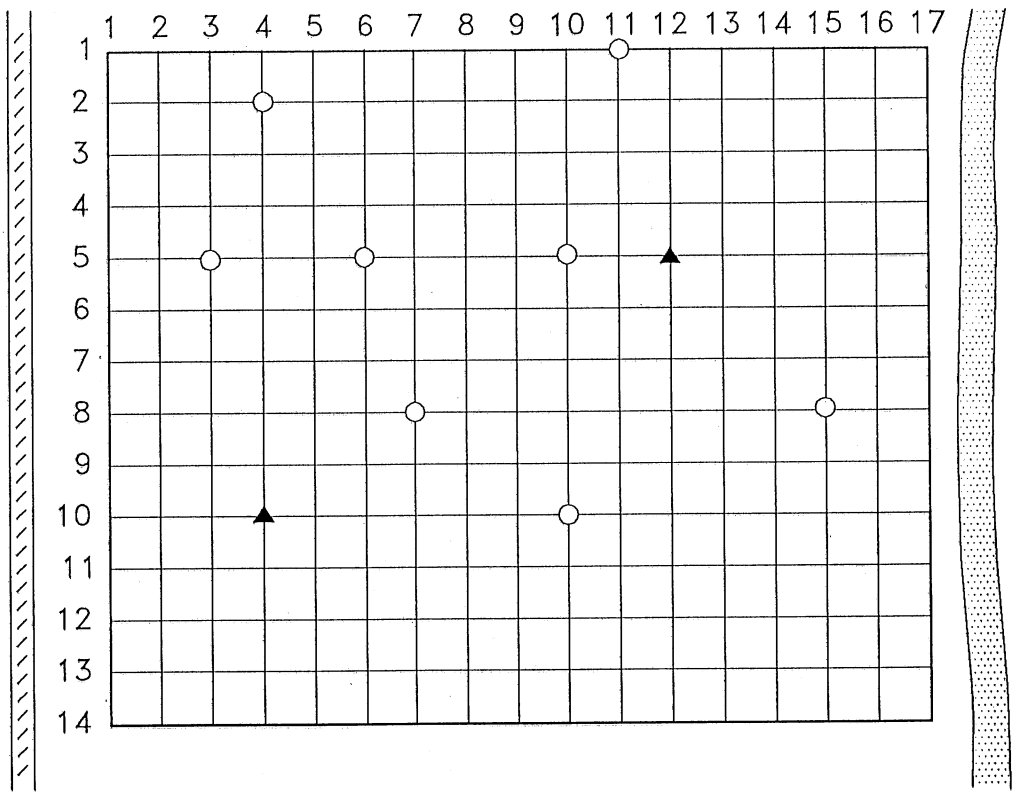

Fig. 16 The alternative with 10 monitoring wells.

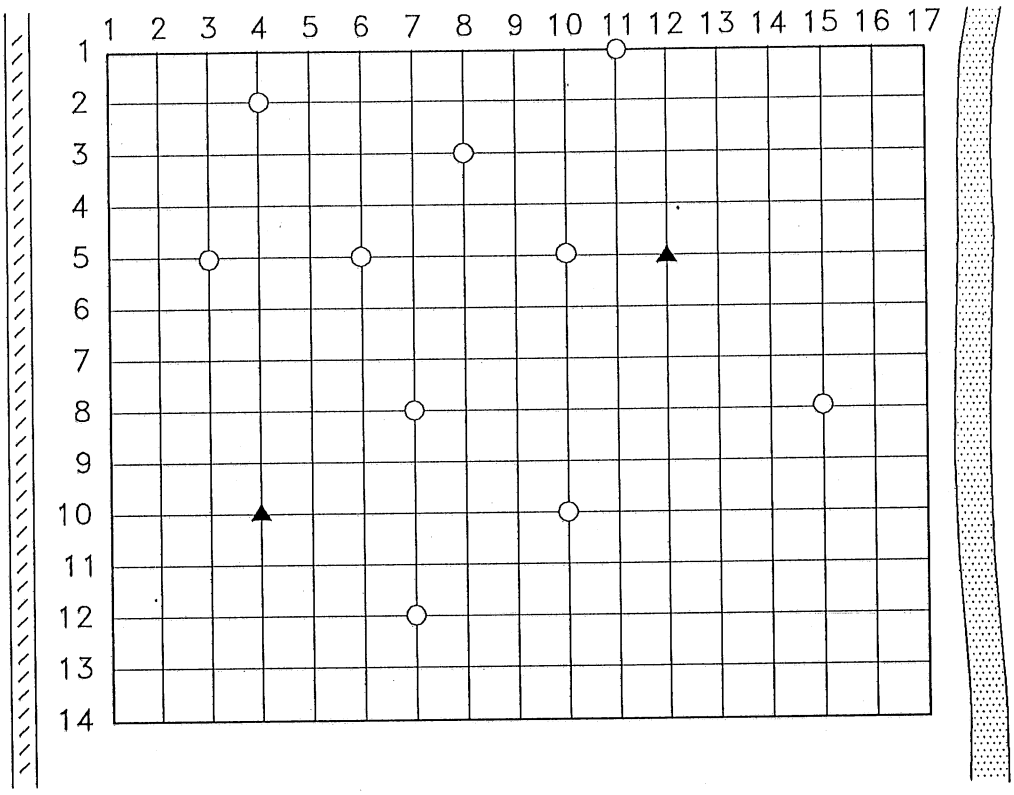

Fig. 17 The alternative with 12 monitoring wells.

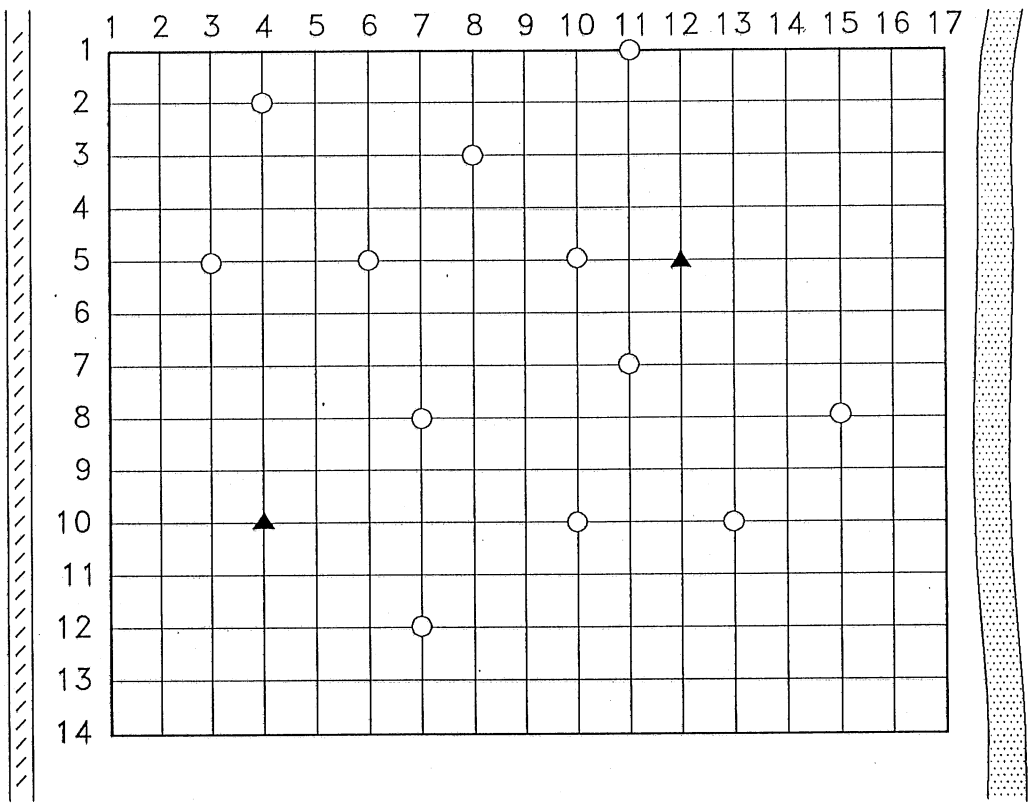

Fig. 18 The alternative with 14 monitoring wells.

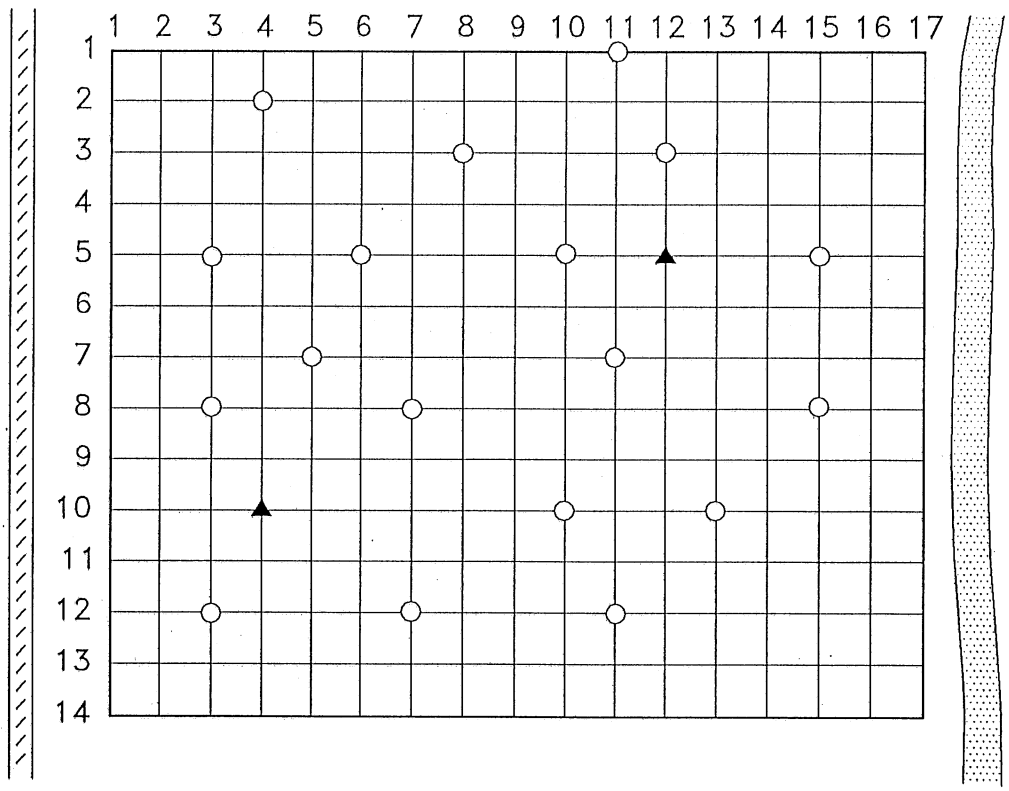

Fig. 19 The alternative with 20 monitoring wells.

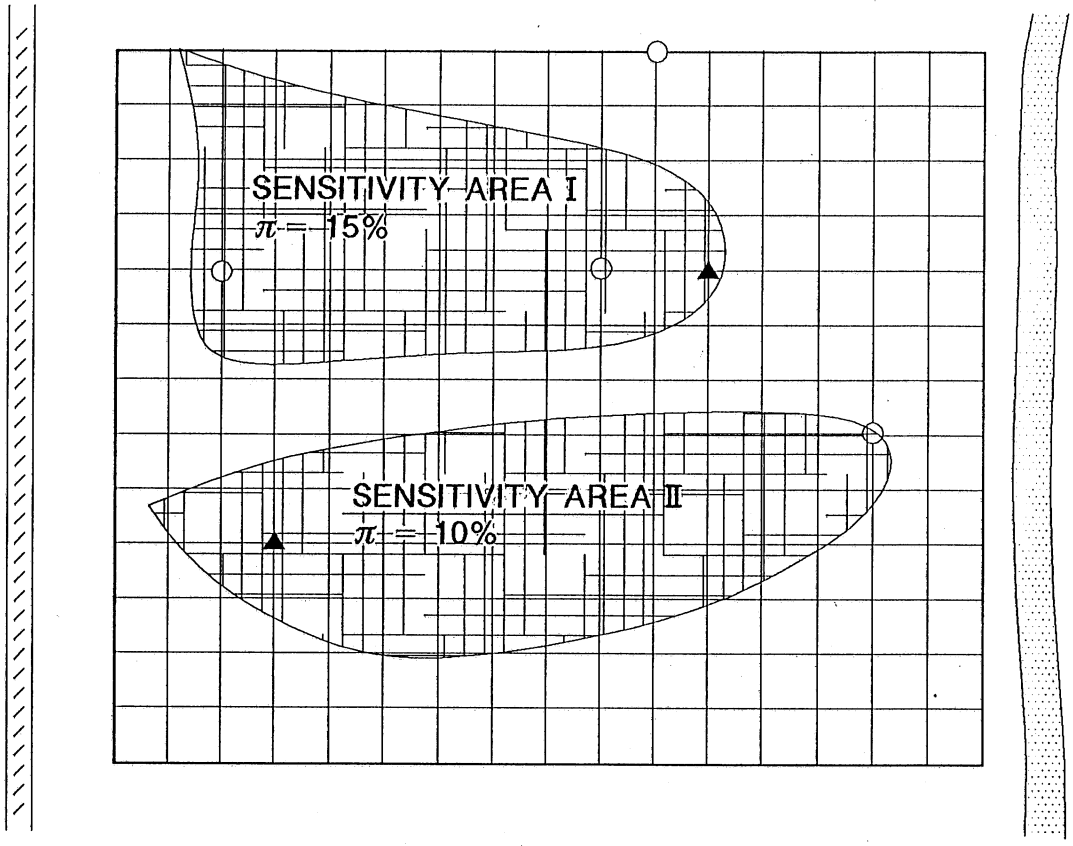

Fig. 20 Two sensitivity areas included in the model under study.

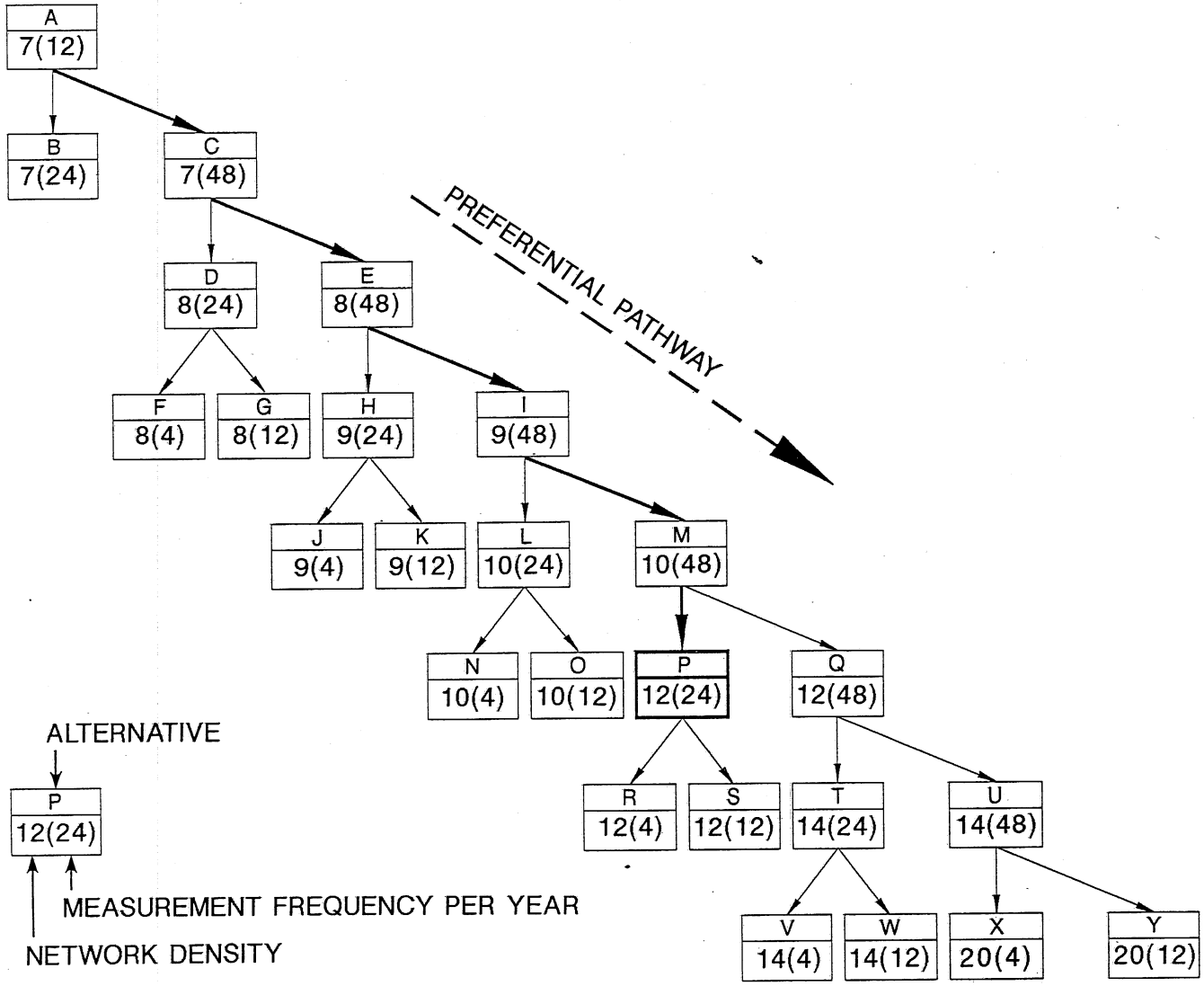

Fig. 21 The search tree for the branch–and–bound algorithm.

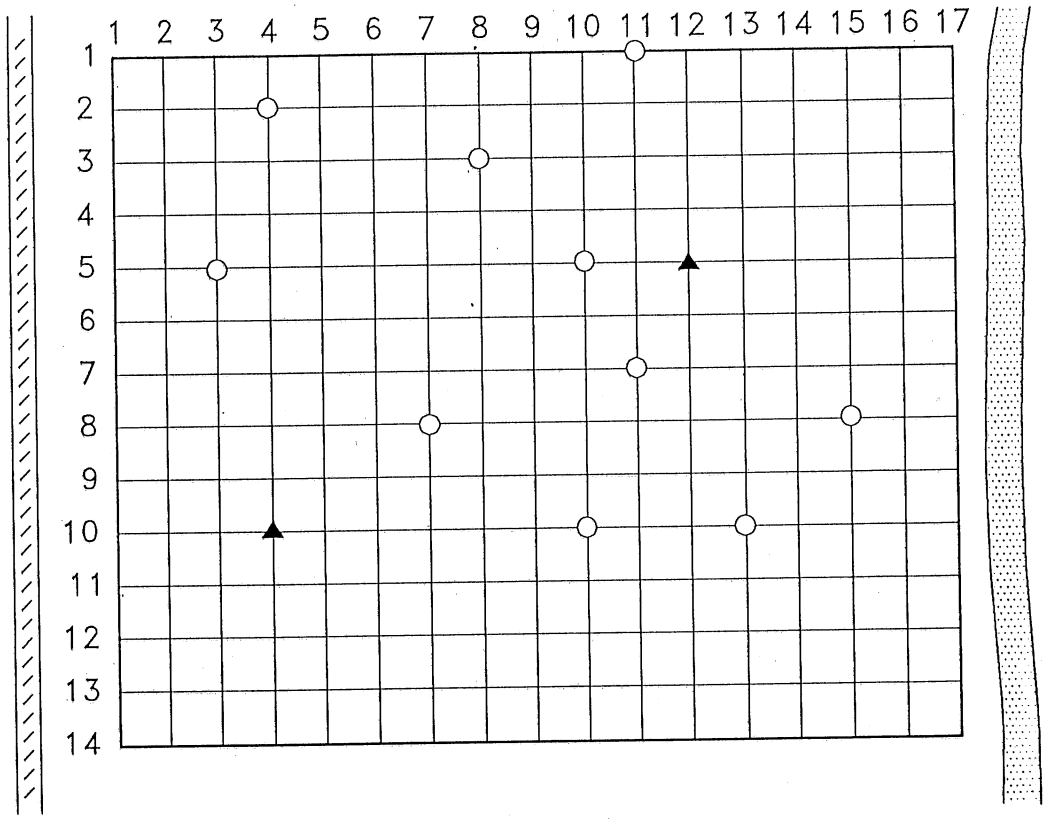

Fig. 22 The optimal monitoring network alternative.

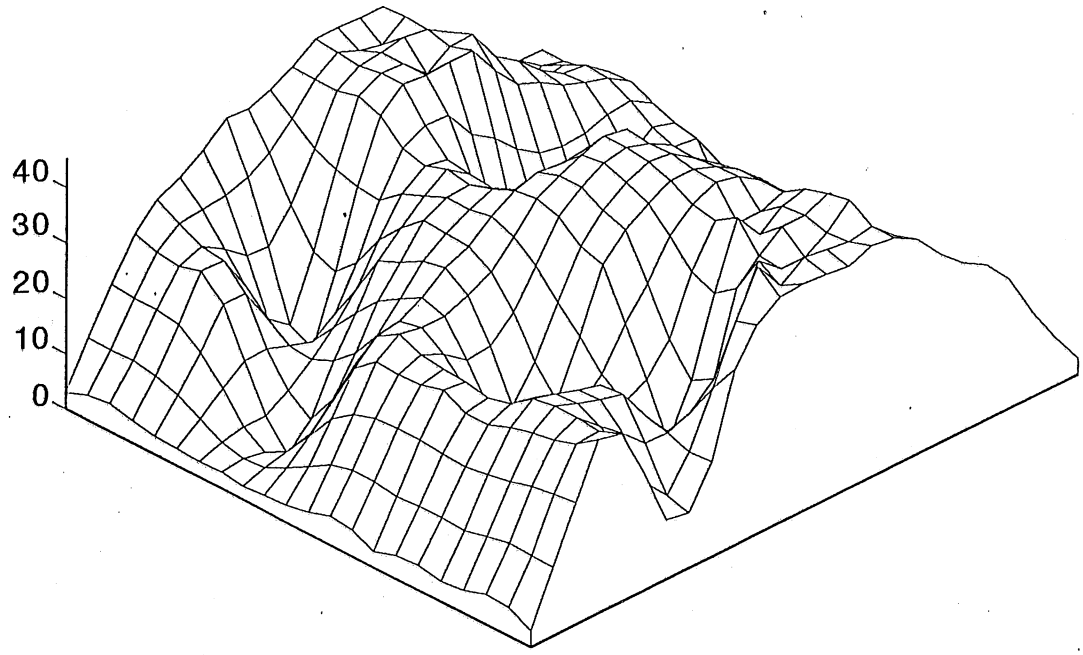

Fig. 23 The error standard deviation surface for the optimal network design.

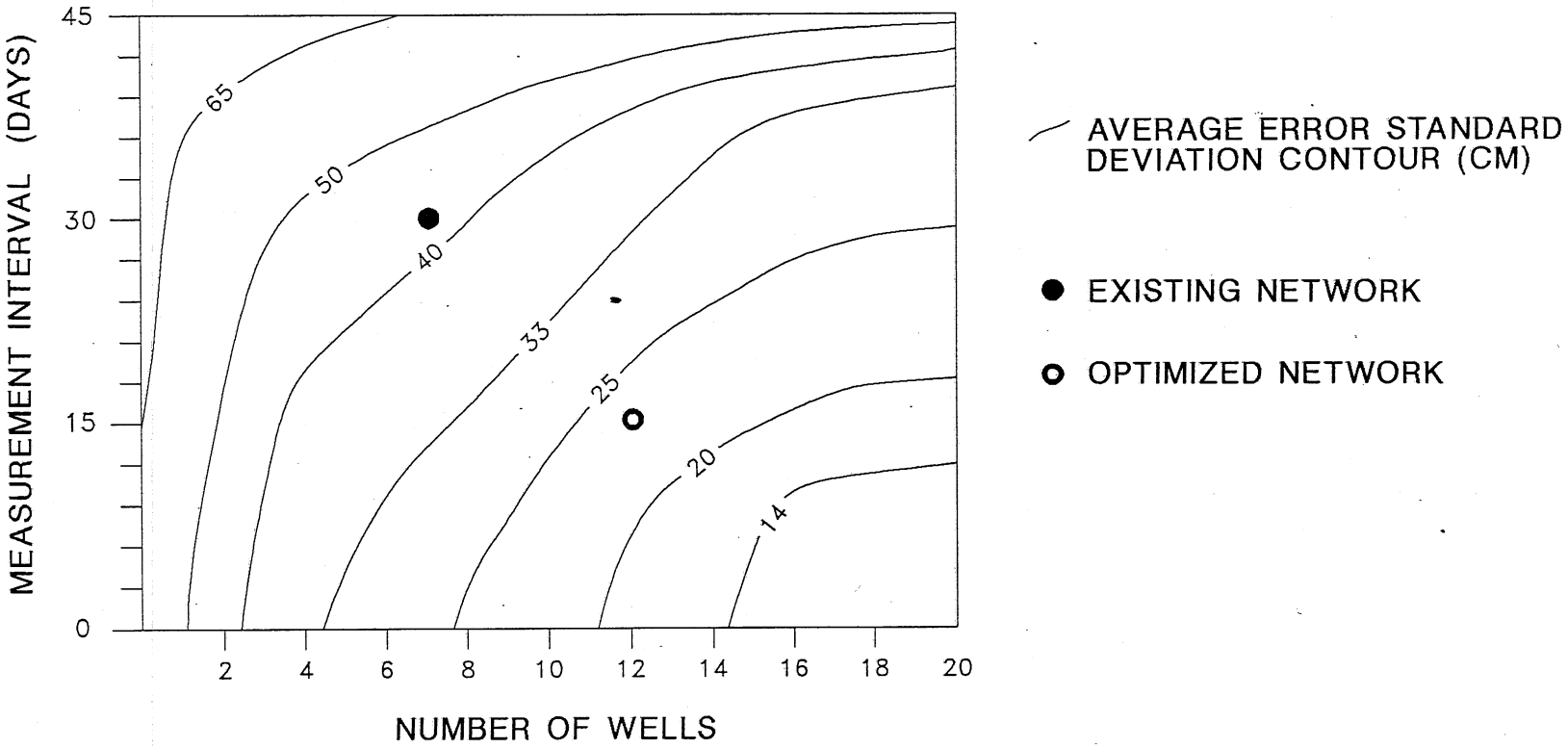

Fig. 24 Space–time tradeoff for the area under study.